MULTI-ENVELOPE PRECODING FOR MASSIVE MIMO SYSTEMS

A THESIS SUBMITTED TO

THE GRADUATE SCHOOL OF ENGINEERING AND SCIENCE

OF BILKENT UNIVERSITY

IN PARTIAL FULFILLMENT OF THE REQUIREMENTS FOR

THE DEGREE OF

MASTER OF SCIENCE

IN

ELECTRICAL AND ELECTRONICS ENGINEERING

By

Mücahit Gümüş

May 2017

Multi-Envelope Precoding for Massive MIMO Systems
By Mücahit Gümüş
May 2017

We certify that we have read this thesis and that in our opinion it is fully adequate, in scope and in quality, as a thesis for the degree of Master of Science.

Tolga Mete Duman (Advisor)

Sinan Gezici

Ayşe Melda Yüksel Turgut

Approved for the Graduate School of Engineering and Science:

Ezhan Karaşan
Director of the Graduate School

ABSTRACT

MULTI-ENVELOPE PRECODING FOR MASSIVE MIMO SYSTEMS

Mücahit Gümüş
M.S. in Electrical and Electronics Engineering
Advisor: Tolga Mete Duman
May 2017

Wireless communications is an important part of information and communication technologies. Particularly, with the introduction of 5G wireless systems, higher data rates, ultra-low latencies and improved power efficiencies are demanded. It is understood that multiple-input multiple-output (MIMO) systems constitute some of the promising technologies to meet these demands, however, currently used number of antennas at the base stations (BS) is not sufficient to reveal the full potential. As a result, massive MIMO systems which use a very large number of antennas at the BSs have recently been proposed as enabling solutions. While massive MIMO promises much for 5G and beyond wireless technologies, there are many problems to be solved including lowering of high built-in and operating costs of BSs to make this technology practical.

Constant envelope (CE) precoding has recently been proposed as a way to reduce the hardware complexity of massive MIMO systems. CE precoding technique for downlink enables a BS structure with one (nonlinear) power amplifier (PA) coupled with continuous or discrete phase shifters in front of each antenna instead of separate highly linear PAs driving each. While CE precoding offers significant reductions in hardware costs, it results in some performance loss in terms of achievable data rates and power efficiencies compared to conventional zero forcing precoding based approaches.

In this thesis, we build on the CE precoding idea and propose the use of a multi-envelope precoding technique for massive MIMO systems which utilizes more than one (but only a few, e.g., 2 or 3) PAs with the objective of recovering some of the performance loss due to the use of CE precoding. The proposed multi-envelope precoding method relies on the standard zero forcing algorithm to group the antennas, and then it utilizes an envelope with a higher level on the antenna group(s) requiring higher power. In other words, the number of power levels used equals to the number of antenna groups. We explore the use of both continuous and discrete phase shifters, and via extensive simulations, we demonstrate that the newly proposed approaches provide significant performance improvements over the CE solutions closing some of the performance gap with average power constraint precoding.

Keywords: Massive MIMO, large scale MIMO, constant envelope precoding, multi-envelope precoding.

ÖZET

BÜYÜK ÇOK GİRDİLİ ÇOK ÇIKTILI SİSTEMLERDE ÇOK GENLİKLİ ÖN KODLAMA

Mücahit Gümüş
Elektrik ve Elektronik Mühendisliği, Yüksek Lisans
Tez Danışmanı: Tolga Mete Duman
Mayıs 2017

Kablosuz iletişim, bilgi ve iletişim teknolojilerinin önemli bir parçasıdır. Özellikle 5G kablosuz iletişim teknolojilerinin takdimi ile birlikte, daha yüksek veri hızları, gelişmiş güç verimliliği ve çok az gecikme süreleri gibi talepler oluşmuştur. Çok girdili çok çıktılı sistemler beklentileri karşılamak yolunda umut veren teknolojilerdendir ancak çok girdili çok çıktılı sistemlerde şu anda kullanılan anten sayıları potansiyeli çıkarmak için çok azdır. Bu yüzden, baz istasyonlarında antenlerin çok miktarda kullanımı olan büyük çok girdili çok çıktılı sistemler çözüm olarak önerilmiştir. Büyük çok girdili çok çıktılı sistemler 5G ve ötesindeki teknolojiler için çok fazla gelişim sunsa da baz istasyonlarının kurulumu ve idame ettirilmesi maliyetlerinin azaltılması gibi çözülmesi gereken çok fazla problem içermektedir.

Kurulum maliyetini azaltmak için iletim durumunda sabit genlikli ön kodlama kullanımı öne sürülmüş ve böylece bir güç yükselteç ve her anten önünde analog veya sayısal faz kaydırıcıları ile baz istasyonu yapısı oluşturulması hedeflenmiştir. Sabit genlikli ön kodlama kurulum maliyetlerinin azaltılması konusunda önemli gelişmeler sunsa da geleneksel sıfır tabanlı kodlama teknikleriyle karşılaştırıldığında başarılabilir veri hızı ve güç verimliliği performanslarında kayıplara neden olmaktadır.

Bu tezde, biz sabit genlikli ön kodlama fikri üzerine dayanarak, başarılabilir veri hızı ve güç verimliliği performanslarındaki kayıpları bir miktar geri kazanmak amacıyla büyük çok girdili çok çıktılı sistemler için birden fazla ancak sayılı nicelikte güç yükselteç kullanımı olan çok genlikli ön kodlama tekniğini sunduk. Çok

genlikli ön kodlama tekniğinde, antenleri gruplamak ve daha yüksek güç ihtiyacı olan antenlerde daha fazla güç tüketmek amacıyla standart sıfır zorlama algoritmasını kullandık. Dolayısıyla her antende aynı genliğin olması yerine anten grubu kadar genlik seviyesi kullandık. Bu kodlama tekniklerinde, analog ve sayısal faz kaydırıcıların olması durumlarını araştırdık ve kapsamlı simülasyonlar kullanarak yeni sunulan yaklaşımın sabit genlikli ön kodlamaya göre önemli performans artışı sağladığını gösterdik.

Anahtar sözcükler: Büyük çok girdili çok çıktılı sistemler, sabit genlikli ön kodlama, çok genlikli ön kodlama.

Acknowledgement

I would like to express my deepest gratitude to my supervisor, Prof. Tolga M. Duman for his great support and guidance throughout the course of this thesis. I appreciate his ideas and comments from which I have learned a lot in the past three years. I also would like to thank Prof. Sinan Gezici and Prof. Melda Yüksel for accepting to serve in my defense committee.

Additionally, I must express my very profound gratitude to my beloved parents for providing me with unfailing support and continuous encouragement throughout my years of study and through the process of researching and writing this thesis. This accomplishment would not have been possible without them. Thank you.

Contents

1 Introduction **2**

1.1 Massive MIMO Systems 4

1.2 Scope of the Thesis 9

2 Preliminaries for Massive MIMO Systems **12**

2.1 System Model 13

2.2 Zero-Forcing Precoding for Massive MIMO Systems 14

2.3 Constant Envelope Precoding for Massive MIMO Systems 15

2.3.1 System Model 16

2.3.2 MUI Analysis 17

2.3.3 CE Precoding Algorithm 18

2.3.4 Achievable Information Sum Rate 22

2.4 Constant Envelope Precoding for Frequency Selective Channels . . . 26
2.4.1 Precoder Design 26
2.4.2 Achievable Information Sum Rate 30
2.5 Chapter Summary 32

3 Multi-Envelope Precoding for Massive MIMO Systems 33
3.1 Multi-Envelope Precoding over Flat Fading Channels 35
3.1.1 Antenna Grouping by Zero-Forcing Precoder 35
3.1.2 Precoder Design 36
3.1.3 Examples 39
3.2 Multi-Envelope Precoding for Massive MIMO Systems over Frequency Selective Channels 47
3.2.1 Antenna Grouping by Using the Zero Forcing Vector 47
3.2.2 Precoder Design 49
3.2.3 Examples 51
3.3 Chapter Summary 53

4 Multi-Envelope Precoding with Digital Phase Shifters for Massive MIMO Systems 54

4.1 Discrete-Phase Constant Envelope Precoding for Massive MIMO Systems . . . 55
4.1.1 System Model . . . 55
4.1.2 Problem Description . . . 55
4.1.3 Trellis Based Constant Envelope Precoding . . . 57
4.1.4 Examples . . . 59
4.2 Discrete-Phase Multi Envelope Precoding for Massive MIMO Systems 61
4.2.1 Antenna Grouping by Zero-Forcing . . . 62
4.2.2 Precoder Design . . . 63
4.2.3 Examples . . . 65
4.3 Chapter Summary . . . 67

5 Conclusions and Future Work 69

List of Figures

1.1 Illustration of different data streams in massive MIMO systems. . . . 6

1.2 Model of RF chain for CE signal transmission from each BS antenna 8

2.1 Illustration of the MUI at each user as a function of the number of BS antennas over Rayleigh fading channel. 21

2.2 The required $\frac{P_{BS}}{\sigma^2}$ ratio versus the number of antennas for a per-user rate of 2 bpcu over a Rayleigh fading channel. 24

2.3 Average achievable data rate (in bpcu) versus the number of antennas over a Rayleigh fading channel. $E_k = P_{BS} = 10$, $\sigma^2 = 1$. 25

2.4 Average achievable data rate (in bpcu) versus the number of BS antennas. $P_{BS} = E_k = 1$, $\sigma^2 = 0.1$, $\tau = 3L$ and $T = 3\tau$. 32

3.1 Multi-envelope precoding block diagram. 34

3.2 BS RF chain with 2 PAs 40

3.3 Average per-user MUI energy versus the number of BS antennas. $p_1 = \sqrt{3/2}$, Rayleigh fading. 41

3.4 Average per-user MUI energy versus the number of BS antennas for varying envelope levels. $M = 24$, Rayleigh fading. 42

3.5 Average per-user MUI energy versus the number of BS antennas for different grouping strategies. $M = 24$, Rayleigh fading. 43

3.6 Average per-user MUI energy versus the number of BS antennas. $M = 24$, Rayleigh fading. 44

3.7 Average per-user MUI energy versus the number of BS antennas for varying envelope levels. $M = 24$, Rayleigh fading. 45

3.8 The required $\frac{P_{BS}}{\sigma^2}$ ratio versus the number of antennas. $M = 40$, Rayleigh fading. 46

3.9 The required $\frac{P_{BS}}{\sigma^2}$ ratio versus the number of BS antennas for $M = 10$ users. 51

4.1 Average achievable data rate (in bpcu) versus the number of antennas for varying set of phase values over Rayleigh fading. $E_k = P_{BS} = 10$, $L = 2$, $M = 10$, $\sigma_w^2 = 1$. 60

4.2 Average achievable data rate (in bpcu) versus the number of BS antennas over Rayleigh fading. $E_k = P_{BS} = 10$, $L = 2$, $M = 10$, $\sigma_w^2 = 1$ 61

4.3 Average achievable data rate (in bpcu) versus the number of BS antennas over Rayleigh fading. $E_k = P_{BS} = 10$, $L = 2$, $M = 10$, $\sigma_w^2 = 1$ 65

4.4 Average achievable data rate (bpcu) versus the number of antennas over Rayleigh fading. $E_k = P_{BS} = 10$, $L = 2$, $M = 10$, $\sigma_w^2 = 1$ 67

List of Tables

3.1 Minimum required P_{BS}/σ^2 (dB) for a given ergodic achievable rate of 2 bpcu. 52

Abbreviations

ADC	analog to digital converter
APC	average only power constraint
AWGN	additive white Gaussian noise
BS	base station
BPCU	bits per channel use
CE	constant envelope
CSI	channel state information
DPC	dirty paper coding
GBC	Gaussian broadcast channel
ISI	inter-symbol interference
LTE	long term evolution
MIMO	multiple input multiple output
MRC	maximal ratio combining
MUI	multi-user interference
MU-MIMO	multi-user multiple input multiple output

NLS	non-linear least squares
NP	non-deterministic polynomial-time
OFDMA	orthogonal frequency division multiple access
PA	power amplifier
PS	phase shifter
SINR	signal to interference and noise ratio
SNR	signal to noise ratio
TB-CEP	trellis based constant envelope precoding
TDD	time division duplex

Chapter 1

Introduction

Wireless communications is an important part of modern information and communication technologies. In particular, the recently defined 5G technologies enable more diverse set of users with different requirements and many new applications such as internet of things demanding higher data rates, ultra-low latencies and higher power efficiencies [1]. Use of massive number of antennas at the base stations (BSs), transmissions using millimeter waves and smaller cell configurations have recently been considered so as to meet these increasing demands [2, 3].

Multiple-input multiple-output (MIMO) systems have been in use for the last few decades, e.g., for a review of their development see [4]. MIMO techniques refer to the use of multiple antennas in transmission and reception of signals which provide significant increase in the channel capacity and/or data reliability. There are different ways to utilize multiple antennas for wireless transmission and reception. For instance, beamforming technique has been used with multiple antennas for a long time in order to increase signal to noise ratio (SNR) by directing radiation [5]. Spatial diversity is another effective technique enabled by MIMO systems to reduce the deleterious effects of wireless channels [4]. Channel coding (i.e., convolutional and block codes, trellis-coded modulation, turbo codes, low-density parity check codes) can be used to provide time diversity over a fading channel [4]. Furthermore, channel coding can be combined with spatial diversity which is provided via MIMO transmission techniques to improve the system performance [4]. For instance, Alamouti scheme exploits the independent fading of channels formed by multiple transmit antenna elements for improved signal fidelity [6]. Through precoding, channel state information (CSI) is exploited to determine the signal in order to minimize the degradation caused by the channel condition [7]. Spatial multiplexing is another technique enabled by MIMO systems which refers to splitting of high rate data to multiple lower rate signals and parallel transmission of each data stream from different antennas [6]. Use of these techniques depends on the knowledge of CSI; for example, if the CSI is known at both of the transmitter and the receiver, spatial multiplexing and precoding can be combined to maximize the system throughput.

Methods of simultaneously transmitting data to several users through the use of multiple antennas is referred as multi-user MIMO (MU-MIMO) techniques. As an example of this set-up, the use of multiple antennas in cellular communications can be given. In MU-MIMO systems, optimal precoding is the subtraction of (non-causally known) interference caused by multi-user communication through a technique called dirty paper coding (DPC) as it has been shown that DPC provides Gaussian broadcast channel (GBC) capacity [8, 9].

The IEEE 802.16e standard uses MIMO techniques and orthogonal frequency division multiple access (OFDMA) together. MIMO systems have also been considered in the 3$^{\text{rd}}$ Generation Partnership Project (3GPP) and Long Term Evolution (LTE) standards [10, 11].

Through utilization of more antennas, a higher number of independent data streams and more degrees of freedom in propagation become available resulting in increased achievable data rates [12]. In addition to these, the BSs equipped with multiple antennas have the capability to focus radiation patterns towards the mobile terminals enhancing the energy efficiency and reducing interference among users. It has recently been shown that these benefits scale up by the use of more antennas at the BSs, however, the current state of the wireless broadband standards such as LTE-Advanced allows for the use of at most 8 antennas [13].

By considering recent demands in wireless communications, and especially the 5G and beyond technologies, scaling up the MIMO and working with more antennas has recently become a popular research topic in communications and signal processing fields [13, 3]. This new approach is called "massive MIMO" or "large-scale MIMO" and it aims to configure communication cells where BSs are equipped with massive number of antennas for serving a high number of mobile terminals simultaneously [2].

1.1 Massive MIMO Systems

Massive MIMO is the scaled up version of MIMO which uses a very large number of antennas at the BSs compared to the current state of art [1, 2]. For example, in a massive MIMO system, a few hundred antennas located at a BS may serve simultaneously tens of terminals using the same time-frequency resource. In 5G technologies, the use of the millimeter wave spectrum is considered for enlarging the frequency band of communication [14]. Recently conducted measurements of indoor and outdoor propagation including path loss values, atmospheric absorption, rain attenuation, reflection coefficients of different objects and building structures at mm-wave spectrum look affirmative and encouraging for the use of mm-waves for wireless communications [14]. In addition, the use of small cells, massive MIMO BS structures and mm-wave spectrum support each other since large number of antennas provide better beamforming capabilities and the use of mm-wave spectrum makes it easier to build large antenna arrays [3]. That is, antenna separation in the order of millimeters is sufficient to provide independent channel realizations.

Some example massive MIMO testbeds have been designed and constructed in [13, 15, 16, 1]. In [1], wireless channel between 4 users and different number of BS antennas (4, 32 and 128) is measured and singular values of the channel matrix are observed to evaluate the difference of the channel responses across different users. In [13], measurement of wireless channel with a large number of antennas (128 cylindrical BS antennas) is realized, and in [16], a linear array of one hundred antennas is built, and this set-up is used for time synchronization, phase coherence and uplink transmission for massive MIMO tests at Lund University. In [15], massive MIMO gains in indoor environments are measured at Rice University with 64 planar antennas.

Massive MIMO systems bring significant capabilities in meeting the demands of 5G and beyond technologies. These capabilities include increase in channel capacity, energy efficiency, reduction of latency and improved robustness against intentional jammers [1, 17, 18].

Thanks to spatial multiplexing and excess degrees of freedom, significant increases in channel capacity are provided via massive MIMO techniques. That is, by using maximal ratio transmission, multi-user interference becomes negligible in comparison to the thermal noise, and many terminals can be served simultaneously. Initial investigations suggest 10 times higher capacity than conventional MIMO systems since many terminals can be served in the same time-frequency resource [1]. Energy can be focused sharply at the locations of terminals by the use of excess number of antennas [19]. Therefore, propagation effects are decreased and energy efficiencies are improved.

When the fading channel to the mobile terminal has a dip (very small gain) due to the distractive additions of signals received via multiple paths, the user needs to wait until the channel changes sufficiently which results in latency [6]. Massive MIMO which is based on beamforming provides channel hardening and eliminates latency [1]. Also, massive MIMO provides excess degrees of freedom which can protect against intentional jammers.

While massive MIMO provides highly significant improvements, there are also some challenges as building these systems necessitate solutions to some newly encountered problems. These problems include difficulties in channel estimation, and potentially high built-in and operational costs of BSs [1, 13].

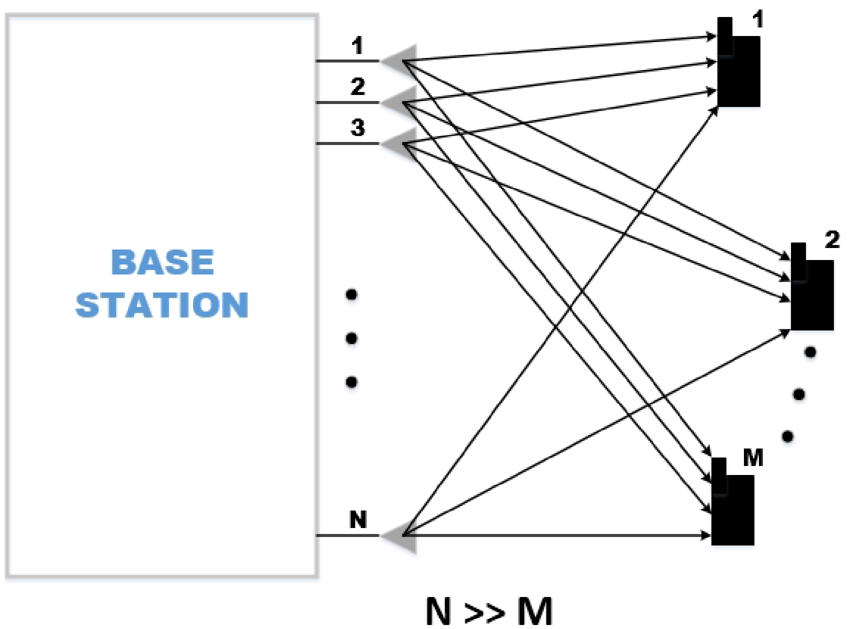

Figure 1.1: Illustration of different data streams in massive MIMO systems.

In wireless communications, channel estimation is generally realized by sending predetermined pilot sequences to a receiver that is by transmitting pilot signals from the BS and estimating the CSI at the mobile users. In a massive MIMO system, however, this is not doable in the downlink direction because of the length of the pilot sequences needed (which is proportional to the number of antennas at the BS) [1]. It is generally considered that the number of antennas is much more than the number of mobile users served as illustrated in Fig. 1.1. Therefore, working in time division duplex (TDD) mode, estimating the channel in the uplink (by sending pilots from the users and estimating the CSI at the BS for each user), and relying on the reciprocity of the channel during the downlink transmission is considered as a feasible method in the literature [20]. Reciprocity of the channel in downlink and uplink directions can be provided by calibration based solutions [1, 21]. However, channel coherence time is limited and allotting a long slot for channel estimation is not desired since it reduces the overall transmission rate. This limits the number of orthogonal pilot sequences used in channel estimation, hence nonorthogonal pilot sequences can be employed by mobile terminals (particularly, by the mobile terminals at different cells). Therefore, pilot signals interfere at the BS resulting in "pilot contamination" [20]. To overcome this problem, many different methods have been considered in the current literature including employment of superimposed pilots, and location and angular discrimination based channel estimation techniques [22, 23, 24]. Well-known methods in estimation theory and signal processing are also applied to solve the channel estimation problem in massive MIMO systems including Bayesian channel estimation and compressive sensing based solutions [25, 26]. Blind pilot decontamination techniques which require shorter pilot sequences is presented in [27, 28].

Due to the use of massive number of antennas at a BS, a very large number of RF components are needed in the BS circuitry. These include highly linear power amplifiers (PAs), phase shifters (PSs), RF switches, analog to digital converters (ADCs), large coaxial cables, etc. [1]. Considering that in conventional schemes, the number of PAs should be equal to the number of RF chains, the PA costs become very high. Further, highly linear power amplifiers are not preferable in terms power efficiency [29]. For instance it is noted that approximately 6 times more power efficient RF components especially PAs are generally nonlinear [29]. Therefore, use of non-linear amplifiers, and decreasing the required number of PAs present themselves as effective solutions to reduce hardware and operational costs. To decrease the number of PAs and to make the nonlinear PAs usable at the BS circuitry, constant envelope (CE) precoding has been proposed in the literature [30, 31, 32]. The idea is the following: in CE precoding, signal amplitudes of all the transmit antennas are picked to be identical, hence utilizing one PA coupled with phase shifters in front of each antenna element is sufficient for implementation as demonstrated in Fig. 1.2. Furthermore, by CE precoding, the use of nonlinear PAs is made possible since only one of them is employed.

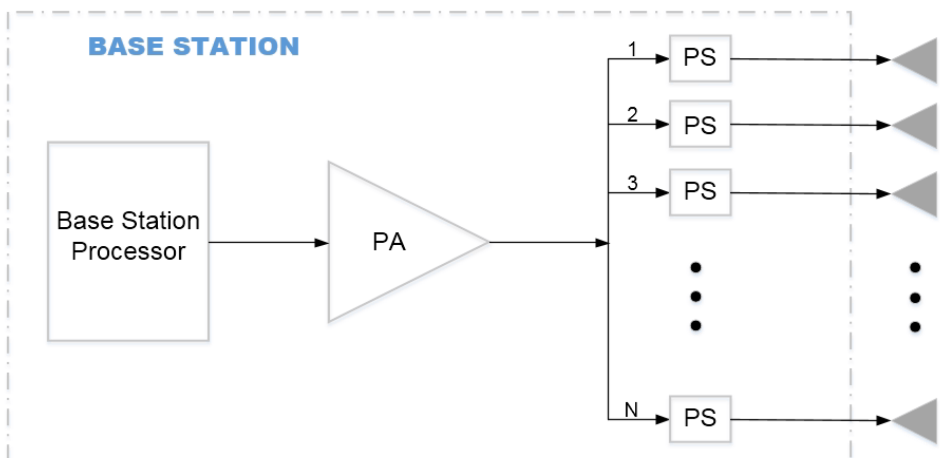

Figure 1.2: Model of RF chain for CE signal transmission from each BS antenna

In order to lower the hardware costs, another idea is to use low precision (e.g., one bit) ADCs since ADC costs and energy consumption increase with the number of precision bits [33]. Maximal ratio combining (MRC), zero forcing (ZF) and least squares (LS) filters have been utilized to analyze one bit ADC performance in massive MIMO systems [33]. It is shown that utilizing one bit ADCs causes significant degradation in data rates in the high SNR regime [33]. Also, channel estimation with the use of pilot sequences is problematic if only one bit ADCs are utilized at the BSs [34]. To recover the performance loss due to the use of one bit ADCs for all antennas, a few antennas are coupled with high-precision ADCs, and most of the antennas are used with one-bit ADCs where the resulting scheme is called as "Mix-ADC" [35]. It is shown that the achievable rate performance of the Mix-ADC scheme is better than the solely low-precision ADC case at the cost of some increase in hardware complexity and energy efficiency. However, it is also noted that other switching algorithms are also required in order to provide the use of high precision ADCs for sampling signals from the antennas having better channel conditions to make the Mix ADC scheme more practical.

As it is explained above, the massive MIMO systems promise much for the next generation and beyond wireless communication technologies, however, there are many challenges that need to be met to make their use practical which motivates the work in this thesis.

1.2 Scope of the Thesis

In this thesis, we focus on hardware complexity of BSs in massive MIMO systems. Specifically, we present multi-envelope precoding techniques which utilize more than one (but only a few, e.g., 2 or 3) PAs at the base stations in order to reduce the performance loss caused by the stringent constraints of CE precoding compared to the average-only power constraint precoding techniques.

In CE precoding, constant envelope complex (low-pass equivalent) signals are transmitted from the BS antennas to simultaneously provide data to mobile terminals by appropriately determining phase values in order to cancel out multi-user interference (MUI) at each user [30]. It is shown that massive MIMO gain and suppression of MUI is still possible under CE precoding assumption even though it is much more restrictive than average only power constraint (APC) precoding techniques [30]. However, the minimum required power in order to provide an achievable rate with CE precoding is greater than the one with APC precoding [30, 31].

Motivated by this observation, we consider the use of a few PAs and employment of different envelopes for different antenna groups instead of a constant envelope for the transmitted signals from all the antennas. We determine the group of antennas requiring higher powers by considering the solution of the zero-forcing algorithm which uses CSI and data vector of all mobile terminals, and assign lower envelopes for antennas requiring lower amplitude signals for the transmission of a given information symbol vector. That is, we perform multi-envelope precoding by considering the CSI and user symbols instead of using a constant envelope for all the antennas. We employ the proposed multi-envelope precoding technique for massive MIMO systems over both flat and frequency selective fading channels.

The use of digital phase shifters which enable a discrete set of phase values in CE precoding scheme for massive MIMO systems is considered in [32]. Through discrete phase shifters, the hardware complexity is decreased and also the system becomes more robust against voltage control line noises [36]. With this motivation, we further extend the newly proposed multi-envelope precoding scheme to the case of discrete phase shifters and develop solutions that utilize trellis based constant envelope precoding (TB-CEP) algorithm of [32]. The TB-CEP algorithm is a multi-stage approach which aims to minimize the objective function whose j-th term depends only on the first j variables. This motivates us to reorder the antennas for the multi-stage solution and to allow for more power on antennas requiring higher envelope signals again by using the zero-forcing solution.

We demonstrate via extensive simulations that the newly proposed multi-envelope precoding techniques provide significant improvements in recovering the performance loss of CE precoding for both cases of discrete and continuous phase shifters. For instance, for a system with 200 antennas serving 40 mobile terminals over a Rayleigh fading channel, the proposed multi-envelope precoding requires around 1 dB less power compared to CE precoding solution to provide an achievable date rate of 2 bits per channel use per user.

The thesis is organized as follows. In Chapter 2, we review the zero-forcing based precoding in massive MIMO systems. We also go over the CE precoding technique for flat and frequency selective fading channels. In Chapter 3, we propose multi-envelope precoding solutions and compare the resulting performances with those of CE precoding. In Chapter 4, we study the use of multi-envelope precoding for massive MIMO systems with discrete-phase shifters at a BS building on the recent proposal of CE precoding with digital phase shifters in [32]. Finally, we conclude the thesis in Chapter 5 with a summary of contributions and suggestions for future research.

Chapter 2

Preliminaries for Massive MIMO Systems

An enabling technology to satisfy the requirements of 5G wireless systems and beyond is massive MIMO as it is recently proven that utilizing a very large number of antennas at a base station increases channel capacity and energy efficiency. A BS equipped with massive MIMO technology can serve many mobile users simultaneously. In such systems, while many users are served, the number of users is still significantly less than the number of antennas on each base station. Despite many advantages offered by these systems, the use of very large number of antennas at a BS brings about some challenges which includes difficulties in channel estimation and increased hardware complexity.

In massive MIMO systems, channel estimation in downlink is a difficult problem because the necessary number of orthogonal pilot sequences is too large due to the need to estimate the channel for each BS antenna. In other words, providing orthogonal pilot sequences requires a long slot for channel estimation, and this causes significant reduction in total data rates since much of the system resources would be spent for estimation purposes. Also, the channel coherence time is limited. Therefore, a reasonable strategy is to estimate the uplink channel at the BS, and rely on channel reciprocity [20]. Although this causes pilot contamination [20] among users the problem becomes much more manageable. After channel estimation, a suitable precoding algorithm is utilized at the BS to combat the channel variations and to cancel out the multi-user interference effects to maximize the system throughput. At the receiver side, the user's data is decoded by using a simple matched filter. In other words, precoding is a crucial step in massive MIMO systems.

In this chapter, we review two topics related to massive MIMO systems which will be used throughout the thesis. We first explain the zero-forcing based precoding approach which uses only an average power constraint. We then review two important papers for the development of this thesis, i.e., [30, 31] for reduced hardware complexity approaches which use only one nonlinear PA in the BS circuitry, i.e., performing constant envelope precoding.

2.1 System Model

A massive MIMO system with a BS equipped with N antennas and serving M single antenna terminals is considered. The channel gain between the k-th user and the n-th BS antenna is denoted by $h_{k,n}$ and the channel vector from all the BS antennas to the k-th user is given by the vector $\mathbf{h_k} = [h_{k,1}, h_{k,2}, ..., h_{k,N}]^T$. The channel matrix between all the BS antennas and all the users is shown by $\mathbf{H} \in \mathbb{C}^{M \times N}$ where the (k, n)-th element of the matrix is $h_{k,n}$. P_{BS} denotes the total transmitted power.

2.2 Zero-Forcing Precoding for Massive MIMO Systems

Zero-forcing (null steering) is a signal processing method which approximately provides interference cancellation hence it approximates the channel capacity if the perfect knowledge of CSI is available at the BS [8, 37]. As high number of antennas are utilized for massive MIMO systems, through the use linear precoding techniques (i.e., zero-forcing precoding, maximal ratio combining), the effects of fast fading and intra-cell multi-user interference (due to the use of orthogonal pilot sequences in a cell) disappear, and only inter-cell interference (with the reuse of pilot sequences at neighboring cells) remains [2]. Let $\mathbf{u}$ be the symbol vector which will be transmitted to the mobile terminals. In matrix form, the relationship between the received signal and the transmit signal for a massive MIMO system is given by

$$\mathbf{y}_{M\times 1} = \mathbf{H}_{M\times N}\mathbf{x}_{N\times 1} + \mathbf{w}_{M\times 1} \tag{2.1}$$

where $\mathbf{w}$ is the white circularly symmetric complex Gaussian noise vector, $\mathbf{x}$ is transmitted signal vector and $\mathbf{y}$ is the received signal vector. The zero-forcing vector is given by

$$\mathbf{z}_f = \mathbf{H}^H(\mathbf{H}\mathbf{H}^H)^{-1}\mathbf{u} \tag{2.2}$$

where $\mathbf{H}^H$ is the Hermitian of channel matrix. Then, the transmitted signal vector becomes

$$\mathbf{x}_{zf} = \alpha\mathbf{z}_f \tag{2.3}$$

where $\alpha = \sqrt{\dfrac{P_{BS}}{{\mathbf{z}_f}^H\mathbf{z}_f}}$. With zero-forcing precoding, the relationship between the received signal and the symbol vector is given by

$$
\begin{aligned}
\mathbf{y}_{zf} &= \mathbf{H}\,\mathbf{x}_{zf} + \mathbf{w} \\
&= \alpha(\mathbf{H}\,\mathbf{H}^H)(\mathbf{H}\,\mathbf{H}^H)^{-1}\,\mathbf{u} + \mathbf{w}, \\
&= \alpha(\mathbf{H}\,\mathbf{H}^H)(\mathbf{H}\,\mathbf{H}^H)^{-1}\,\mathbf{u} + \mathbf{w}, \\
&= \alpha\,\mathbf{u} + \mathbf{w}.
\end{aligned}
\tag{2.4}
$$

In other words, the noise-free received signal $(\mathbf{y}_{zf} - \mathbf{w})$ is a scaled version of the information symbol vector which means that the interference due to the simultaneous transmissions is canceled out as we consider a single cell scenario.

While zero-forcing technique is highly effective, one downside is the need for large variations among the signal amplitudes of different antennas which is only possible with the use of N highly linear (and very expensive) power amplifiers in the BS circuitry [1, 30].

2.3 Constant Envelope Precoding for Massive MIMO Systems

One way to decrease the hardware complexity of massive MIMO systems is to utilize constant envelope (CE) precoding in transmission. In CE precoding, the use of only one (nonlinear) PA coupled with phase shifters in front of each antenna element is sufficient as the CE signal is generated by varying only the phase of the constant amplitude baseband signals providing significant savings in complexity.

A natural question that arises with the use of CE precoding is whether the multi-user interference (MUI) suppression and effective array gain can still be achieved or not. Different from the solutions with APC, the CE precoding is highly restrictive as does not allow for variations among the signal levels of different antennas. In

[30], the CE precoding scheme is considered with the objective of minimizing the MUI at each user. When information symbols for each user and the channel state information (CSI) between the base station (BS) and users is given, constant envelope signals are determined in such a way that the MUI energy at each user is made as small as possible. In this section, we explain the CE precoding algorithm of [30] for massive MIMO systems under flat fading channels and illustrate the performance of the scheme via simulations.

2.3.1 System Model

With the CE constraint, the power transmitted from each antenna becomes P_{BS}/N. Then, it is clear that signal from the n-th BS antenna is given by $x_n = \sqrt{P_{BS}/N} e^{j\theta_n}$ where θ_n is the phase angle of the constant envelope signal. We define $\boldsymbol{\theta} = [\theta_1, \theta_2, ..., \theta_N]^T$ as the phase angle vector.

When constant envelope signals are transmitted from the BS antennas, the signal received at the k-th user is given by

$$y_k = \sqrt{P_{BS}/N} \sum_{n=1}^{N} h_{k,n} e^{j\theta_n} + w_k, k = 1, 2, ..., M. \tag{2.5}$$

Here, $w_k \sim CN(0, \sigma^2)$ is the circularly symmetric complex Gaussian noise at the k-th user. Let $u_k \in U_k$ (where U_k is the unit energy information alphabet) represent the normalized symbol which is transmitted to k-th user and, E_k be the symbol energy for $k = 1, 2, ..., M$. Then, $\mathbf{u} = [\sqrt{E_1} u_1, ..., \sqrt{E_M} u_M]^T$ is the scaled information symbol vector and $\mathcal{U} \triangleq \sqrt{E_1} U_1 \times \sqrt{E_2} U_2 \times ... \times \sqrt{E_M} U_M$ is the fixed scaled information symbol library for all the users.

2.3.2 MUI Analysis

With the transmission phase angle vector $\boldsymbol{\theta}$, and u_k denoting the information symbol to the k-th user, using (2.5), the received signal at the k-th user can be expressed as

$$y_k = \sqrt{P_{BS}}\sqrt{E_k}u_k + \sqrt{P_{BS}}s_k + w_k, \tag{2.6}$$

where

$$s_k = \frac{\sum_{n=1}^{N} h_{k,n} e^{j\theta_n}}{\sqrt{N}} - \sqrt{E_k}u_k$$

Here, $\sqrt{P_{BS}}s_k$ is the MUI term in the received signal. As proved in [30], the MUI term vanishes as the number of antennas goes to infinity. This behavior can be explained as follows. By using (2.6), the noise-free received signal after dividing with P_{BS} can be expressed as

$$f_k = \frac{\sum_{n=1}^{N} h_{k,n} e^{j\theta_n}}{\sqrt{N}}, \theta_n \in [-\pi, \pi), n = 1, 2, ..., N. \tag{2.7}$$

Then, the range of noise free signals that can be received by the users generate a set, $\mathcal{M}(\mathbf{H})$ where any vector $\mathbf{f} = [f_1, ..., f_M] \in \mathcal{M}(\mathbf{H})$. In other words, any $\mathbf{f}$ can be expressed by at least one $\boldsymbol{\theta}^f = [\theta_1^f, ..., \theta_N^f]$. Let the N/M be integral without loss of generality. Then, the summation on $\boldsymbol{\theta}^f$ can be expressed as a sum of N/M terms.

$$f_k = \sum_{i=1}^{N/M} v_k^i, v_k^i \triangleq \frac{1}{\sqrt{N}} \left(\sum_{l=(i-1)M+1}^{iM} h_{k,l} e^{j\theta_l^f} \right), i = 1, ..., \frac{N}{M}. \tag{2.8}$$

In this expression, each term of the summation is topologically similar since all the channel gains between the BS antennas and the users have the same statistical properties, and under some mild conditions, $\mathcal{M}(\mathbf{H})$ expands if N increases. However, the volume is fixed since the BS power is constant so the set $\mathcal{M}(\mathbf{H})$ becomes denser with increasing N [30]. In other words, with fixed M and E_k values, increasing N sufficiently large provides a nonzero probability for any vector $\mathbf{f} \in \mathcal{M}(\mathbf{H})$ which is very close to $\mathbf{u} = [\sqrt{E_1}u_1, ..., \sqrt{E_M}u_M]$ in terms of Euclidean distance. Therefore, increasing N while M and E_k are fixed provides with reduction in the MUI energy at each user.

2.3.3 CE Precoding Algorithm

Signal envelope is constant so the precoder in this setup only aims to choose the $\boldsymbol{\theta}$ vector which decreases the MUI energy at each user in order to enable reliable communication between the BS and mobile terminals. This problem can be formulated as a non-linear least squares (NLS) optimization problem, i.e.,

$$\boldsymbol{\theta}^{\boldsymbol{u}} = [\theta_1^u, ..., \theta_N^u]^T = \underset{\theta_i \in [-\pi,\pi), i=1,...,N}{\operatorname{argmin}} g(\boldsymbol{\theta}, \mathbf{u}), \tag{2.9}$$

where

$$\begin{aligned} g(\boldsymbol{\theta}, \mathbf{u}) &\triangleq \sum_{k=1}^{M} |s_k|^2 \\ &= \sum_{k=1}^{M} \left| \frac{\sum_{n=1}^{N} h_{k,n} e^{j\theta_n}}{\sqrt{N}} - \sqrt{E_k} u_k \right|^2 . \end{aligned}$$

Although the NLS problem in (2.9) is non-convex and it has many local minima, it has been observed in [30] that its solution at most local minima is small enough if the ratio of N/M is high, that is, if a large number of degrees of freedom is available. Also, a fast iterative algorithm has been proposed to solve this problem in [30] (which is summarized in Algorithm 1).

In Algorithm 1, there are N sub-iterations in each iteration. Let "p" denote the iteration count and "q" be the subiteration count. If $q = N$, algorithm moves to the $(p + 1, q)$-th iteration. Otherwise, it moves to the $(p, q + 1)$-th iteration. Let $\boldsymbol{\theta}^{p,q}$ be

Algorithm 1 Iterative CE precoding algorithm for massive MIMO systems.

1. $\boldsymbol{\theta} = \mathbf{0}$
2. **for** $iter = 1$ to $iterationCount$ **do**
3.   **for** $i = 1$ to N **do**
4.   Calculate interference on each user by neglecting the signal from the i-th antenna
5.   Multiply it with the Hermitian of the channel from i-th antenna to that user.
6.   Sum the resulting term for all users.
7.   Get the argument of the summation.
8. $\boldsymbol{\theta_i} = \pi + argument$
9.   **end for**
10. **end for**

the set of angles after the q-th subiteration of the p-th iteration. Then, keeping all the other phase angles the same as the previous subiteration, $\boldsymbol{\theta}^{p,q+1}$ is

$$\begin{aligned}\boldsymbol{\theta}^{(\boldsymbol{p},\boldsymbol{q}+\mathbf{1})} &= \underset{\boldsymbol{\theta}=\theta_1^{(p,q)},...\theta_q^{(p,q)},\phi,\theta_{q+2}^{(p,q)},...,\theta_N^{(p,q)},\phi\in[-\pi,\pi)}{\text{argmin}} g(\boldsymbol{\theta},\mathbf{u}),\\ &= \pi + arg\left(\sum_{k=1}^{M} \frac{h_{k,q+1}^{*}}{\sqrt{N}}\left[\left(\frac{1}{\sqrt{N}}\sum_{n=1,\neq q+1}^{N} h_{k,n}e^{j\theta_n^{(p,q)}}\right)-\sqrt{E_k}u_k\right]\right) \qquad (2.10)\\ \theta_i^{(p,q+1)} &= \theta_i^{(p,q)}, i=1,2,...,N, i\neq q+1.\end{aligned}$$

The number of iterations in Algorithm 1 is selected much smaller than N, and each iteration includes N subiterations. Therefore, the complexity of the algorithm to compute all N transmit phase angles is $O(MN)$. Denoting the phase angles after the last iteration as $\hat{\boldsymbol{\theta}}^{u} = [\hat{\theta_1}^{u}, ..., \hat{\theta_N}^{u}]^T$, the MUI at the k-th user is expressed as follows

$$\hat{s}_k = \left(\frac{\sum_{n=1}^{N} h_{k,n}e^{j\hat{\theta}_n^u}}{\sqrt{N}} - \sqrt{E_k}u_k\right). \qquad (2.11)$$

By using this expression, the signal to interference and noise ratio (SINR) at the k-th user is given by

$$\gamma_k(\mathbf{H},\mathbf{E},\frac{P_{BS}}{\sigma^2}) = \frac{E_k}{\mathbb{E}_{u_1,...,u_M}[|\hat{s}_k|^2] + \dfrac{\sigma^2}{P_{BS}}} \qquad (2.12)$$

where $\mathbf{E} \triangleq [E_1, ..., E_M]^T$ is the vector of symbol energies of all users and $\mathbb{E}_{u_1,...,u_M}[|\hat{s}_k|^2]$ is the expected value of MUI energy over normalized user symbols. It is desired to have a low MUI at each receiver which corresponds to a larger SINR value and hence an increased data rate.

An example is provided in Fig. 2.1. The channels are assumed to be independent Rayleigh fading, the codebooks are assumed to be complex Gaussian for all the users with $U_1 = U_2 = ... = U_M = CN(0,1)$, and $E_1 = E_2 = ... = E_M = 1$ are picked. The figure illustrates the resulting MUI energy averaged over the channel statistics, i.e., $\mathbb{E}_{\mathbf{H}}[|\hat{s}_k|^2]$.

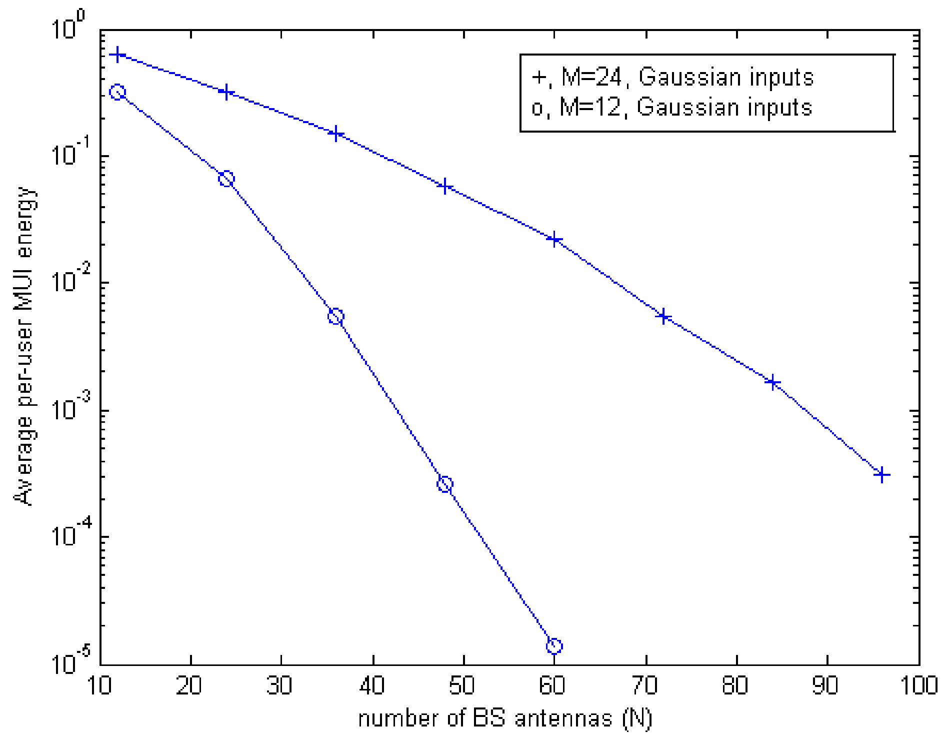

Figure 2.1: Illustration of the MUI at each user as a function of the number of BS antennas over Rayleigh fading channel.

It is observed that for a fixed information symbol energy and number of users, the average MUI energy decreases with increasing the number of BS antennas. To increase the SINR level further, from (2.12), it is obvious that information symbol energy, E_k, for each user should be increased and MUI energies at each user should be kept sufficiently small which is possible by increasing N and E_k proportionally. It is inferred through Fig. 2.1 that the per user ergodic MUI energy can be kept small if E_k increases with increasing N. Furthermore, it is possible to decrease P_{BS} while keeping a constant received SINR level if N and E_k increases accordingly since noise effect $\dfrac{\sigma^2}{P_{BS}}$ increases with reduction in total transmit power P_{BS} as in (2.12).

2.3.4 Achievable Information Sum Rate

In this section, an ergodic information sum rate is given for the proposed CE pre-coding algorithm (developed in [30]). We denote the mutual information by I and differential entropy for continuous random variables by h. When the information alphabet, $U_1 = ... = U_M$, information symbol energy, $E_1, ...E_M$, and total BS transmit power to noise ratio, $\frac{P_{BS}}{\sigma^2}$ are fixed, the mutual information expression between y_k and u_k becomes

$$\begin{aligned} I(y_k, u_k) &= h(u_k) - h(u_k|y_k) \\ &= h(u_k) - h\left(u_k - \frac{y_k}{\sqrt{P_{BS}}\sqrt{E_k}} \middle| y_k \right) \\ &\geq h(u_k) - h\left(u_k - \frac{y_k}{\sqrt{P_{BS}}\sqrt{E_k}} \right) \end{aligned} \tag{2.13}$$

where the second line follows as the subtracted term only includes the conditioned random variable, and the third line follows since conditioning is removed. After combining (2.11) and (2.13), it can be shown that a lower bound on the mutual information for the k-th user is given by

$$I(y_k, u_k) \geq h(u_k) - h\left(\frac{\hat{s}_k}{\sqrt{E_k}} + \frac{w_k}{\sqrt{P_{BS}}\sqrt{E_k}} \right) \tag{2.14}$$

where u_k is a complex random variable with unit variance, denoting the k-th user's information symbol. We select it as a complex Gaussian random variable to maximize the right hand side resulting in

$$I(y_k, u_k) = log_2(\pi e) - h\left(\frac{\hat{s}_k}{\sqrt{E_k}} + \frac{w_k}{\sqrt{P_{BS}}\sqrt{E_k}} \right) \tag{2.15}$$

Since differential entropy is maximized with complex Gaussian random variables (under a power constraint), the largest value for the second term on the right hand side can be obtained as $log_2\left(\pi e \, var\left[\frac{\hat{s}_k}{\sqrt{E_k}} + \frac{w_k}{\sqrt{P_{BS}}\sqrt{E_k}} \right] \right)$ resulting in a lower bound to mutual information given by

$$I(y_k, u_k) \geq log_2(\pi e) - log_2\left(\pi e \, var\left[\frac{\hat{s}_k}{\sqrt{E_k}} + \frac{w_k}{\sqrt{P_{BS}}\sqrt{E_k}} \right] \right). \tag{2.16}$$

where var is variance operator. Noting that $\mathbb{E}[|\mathbf{X}|^2] \geq var(\mathbf{X})$ for any complex random variable $\mathbf{X}$, we can further write

$$
\begin{aligned}
I(y_k, u_k) &\geq log_2(\pi e) - log_2\Bigg(\pi e\, \mathbb{E}\Bigg[\Bigg|\frac{\hat{s}_k}{\sqrt{E_k}} + \frac{w_k}{\sqrt{P_{BS}}\sqrt{E_k}}\Bigg|^2\Bigg]\Bigg) \\
&= log_2(\pi e) - log_2\Bigg(\pi e\, \frac{\mathbb{E}|\hat{s}_k|^2}{E_k} + \frac{\sigma^2}{P_{BS}E_k}\Bigg) \\
&= log_2\Bigg(\gamma_k(\mathbf{H}, \mathbf{E}, \frac{P_{BS}}{\sigma^2})\Bigg)
\end{aligned}
\tag{2.17}
$$

Clearly, $R_k(\mathbf{H}, E, \frac{P_{BS}}{\sigma^2}) = log_2\Bigg(\gamma_k(\mathbf{H}, \mathbf{E}, \frac{P_{BS}}{\sigma^2})\Bigg)$ is an achievable information rate.

By adding the achievable rates of all the users $R_k(\mathbf{H}, E, \frac{P_{BS}}{\sigma^2})$ and averaging over the channel statistics, an ergodic information sum rate for this set-up is obtained as

$$
R^{CE}\left(\mathbf{E}, \frac{P_{BS}}{\sigma^2}\right) \triangleq \sum_{k=1}^{M} \mathbb{E}_{\mathbf{H}}\Bigg[R_k(\mathbf{H}, \mathbf{E}, \frac{P_{BS}}{\sigma^2})\Bigg]. \tag{2.18}
$$

The system being considered is nothing but a Gaussian broadcast channel (GBC). The ergodic information sum rate for this GBC with CE precoding can be further optimized on the energies picked for each user. Assuming that $E_1 = E_2 = ... = E_M = \hat{E}$ and that all the users have the same information alphabet as in (2.19), we can optimize this rate over the energy value $\hat{E}$, i.e., the achievable rate becomes

$$
R^{CE}\left(\frac{P_{BS}}{\sigma^2}\right) \triangleq \max_{\mathbf{E}\,|\,E_1=E_2=...=E_M=\hat{E}>0} R^{CE}\left(\mathbf{E}, \frac{P_{BS}}{\sigma^2}\right). \tag{2.19}
$$

As an example, we illustrate the minimum power requirement for a given achievable bit per channel use (bpcu) rate in Fig. 2.2. The channels are assumed to be independent Rayleigh fading, the codebooks are complex Gaussian for all the users with $U_1 = U_2 = ... = U_M = CN(0, 1)$. Maximization in (2.19) is performed numerically by varying $\hat{E}$. The figure illustrates the required minimum $\frac{P_{BS}}{\sigma^2}$ values for an achievable rate level $R^{CE}\left(\frac{P_{BS}}{\sigma^2}\right)$.

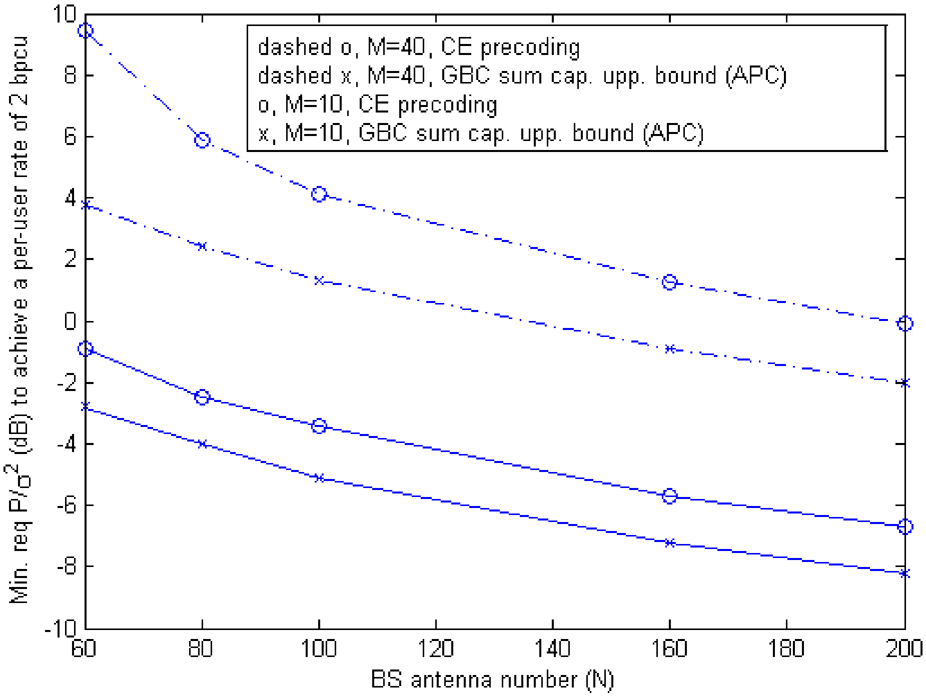

Figure 2.2: The required $\dfrac{P_{BS}}{\sigma^2}$ ratio versus the number of antennas for a per-user rate of 2 bpcu over a Rayleigh fading channel.

In order to compare the performance of CE precoding with that of APC precoding, the cooperative upper bound on the GBC sum-capacity is also plotted [30, 38]. We observe in Fig. 2.2 that there is a gap between the achievable rates with APC and CE precoding solutions. For example, for large number of antennas, the gap between the APC precoding and CE precoding is only around 1.7 dB. This is remarkable since the constant envelope constraint is much more restrictive than the average only power constraint. Further, it is demonstrated that the array gain is maintained with the CE constraint, i.e., the required $\dfrac{P_{BS}}{\sigma^2}$ level decreases by 3 dB with the use of twice as many BS antennas.

We report the simulated achievable transmission rates in bits per channel use

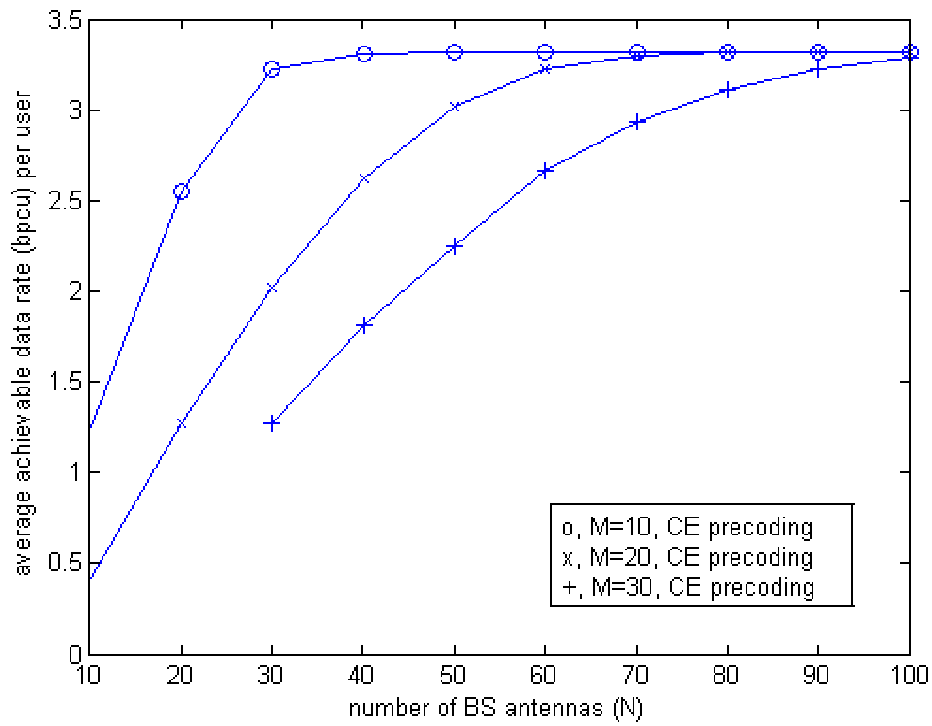

Figure 2.3: Average achievable data rate (in bpcu) versus the number of antennas over a Rayleigh fading channel. $E_k = P_{BS} = 10$, $\sigma^2 = 1$.

versus the number of BS antennas for different number of users in Fig. 2.3. It is observed that when the symbol energy and the average power of BS are fixed, increasing the number of BS antennas provides improvements in per user achievable information rates as expected. This is because increasing the number of BS antennas while the symbol energies are kept fixed results in reduction in the MUI energy. Also, it is observed that after some point, the MUI becomes negligible compared to the AWGN level, hence increasing the number of antennas beyond this point does not offer any further significant improvements in the resulting achievable information rates.

2.4 Constant Envelope Precoding for Frequency Selective Channels

The CE precoding technique which can be used for flat fading channels as in [30] is further adapted to massive MIMO systems with frequency selective fading in [31]. Frequency selective discrete-time complex baseband channel between the n-th BS antenna and the k-th user is modeled as a finite impulse response filter of length L with the tap coefficients $h_{k,n}[0], h_{k,n}[1], ..., h_{k,n}[L-1]$. Let $\boldsymbol{\theta}[t] = [\theta_1[t], \theta_2[t], ..., \theta_N[t]]^T$ be the phase angle vector for time t, then the signal received at the k-th user at time t is written as

$$y_k[t] = \sqrt{\frac{P_{BS}}{N}} \sum_{n=1}^{N} \sum_{l=0}^{L-1} h_{k,n}[l] e^{j\boldsymbol{\theta}_n[t-l]} + w_k[t] \tag{2.20}$$

where $w_k[t]$ denotes the complex Gaussian noise term.

2.4.1 Precoder Design

The channel is frequency selective, hence there is inter-symbol interference (ISI) between consecutive L received symbols as shown in (2.20). This is why, the idea of CE precoding approach developed for flat fading channel case cannot be applied directly to this setup. That is, the transmit phase angles at a time instance cannot be solved independently of the previous angles used. Therefore, a blockwise transmission scheme is considered. The data transmission period at the downlink direction following a channel estimation slot can be considered as the precoding block. This necessitates determination of phase angles of all the antennas for an entire coherence time, T, after the channel estimation period. In this manner, there is no ISI between consecutive blocks since the ISI terminates during channel estimation phase.

For a given CSI and symbol sequence to be transmitted in a given coherence interval denoted by $\mathbf{u}[1], \mathbf{u}[2], ..., \mathbf{u}[T]$, the transmission phase angles are calculated via the following optimization problem:

$$[\boldsymbol{\theta}^u[1], \boldsymbol{\theta}^u[2], ..., \boldsymbol{\theta}^u[T]] = \underset{\theta^u_{n,t} \in [-\pi,\pi), t=1,2,...,T, n=1,2,...,N}{\operatorname{argmin}} \sum_{t=1}^{T} \sum_{k=1}^{M} \left| \frac{\sum_{n=1}^{N} \sum_{l=0}^{L-1} h_{k,n}[l] e^{j\theta_n[t-l]}}{\sqrt{N}} - \sqrt{E_k} u_k[t] \right|^2 \tag{2.21}$$

There are a large number of optimization variables in this problem, hence the complexity is much higher than that of the flat fading case. This is why, it is proposed to split the transmission block into several subblocks which will simplify the problem. This splitting idea is heuristic and there is no proof about its optimality, however, extensive simulation results have shown its excellent performance in [31].
Length of transmission blocks, τ, which is much less than T and much greater than L is reasonable to provide both an acceptable complexity and proportionally less degradation in the system performance. If the MUI terms are split into blocks of length, τ, the optimization problem in (2.21) becomes

$$\begin{aligned}
[\boldsymbol{\theta}^u[1], \boldsymbol{\theta}^u[2], ..., \boldsymbol{\theta}^u[T]] &= \underset{\theta^u_{n,t} \in [-\pi,\pi), t=1,2,...,T, n=1,2,...,N}{\operatorname{argmin}} \sum_{r=1}^{\lceil T/r \rceil} I_r, \\
I_r \triangleq f(\boldsymbol{\theta}[(r-1)T-L+2], ..., &\boldsymbol{\theta}[min(T, r\tau)], \mathbf{u}[(r-1)T+1], ..., \mathbf{u}[min(T, r\tau)]) \\
&= \sum_{t=(r-1)\tau+1}^{min(T,r\tau)} \sum_{k=1}^{M} \left| \frac{\sum_{n=1}^{N} \sum_{l=0}^{L-1} h_{k,n}[l] e^{j\theta_n[t-l]}}{\sqrt{N}} - \sqrt{E_k} u_k[t] \right|^2
\end{aligned} \tag{2.22}$$

In this problem, there are T/τ optimization blocks. I_r denotes the r-th block which is a function of $\boldsymbol{\theta}^r \triangleq (\boldsymbol{\theta}[(r-1)\tau+1]^T, ..., \boldsymbol{\theta}[min(T, r\tau)]^T)^T$, and it also depends on the phase angles transmitted at the time instances $(r-1)\tau - L + 2, ..., (r-1)\tau$ (in the previous block). The CE precoding is applied sequentially. I_1 is solved independently, and I_2 is solved by knowing the last $L-1$ phase vectors of I_1, and continuing in this manner until the last block is solved, and the CE precoding operation for the entire coherence time is completed.

An iterative algorithm to solve for the phases of the r-th block is proposed in [31] is summarized in Algorithm 2.

Algorithm 2 Iterative CE precoding algorithm for massive MIMO systems over frequency selective channels.

---

1. $\mathbf{\Theta} = \mathbf{0}_{N \times T}$
2. **for** $iter = 1$ to $iterationCount$ **do**
3.   **for** $t = (r-1)\tau + 1$ to $min(r\tau, T)$ **do**
4.   **for** $n = 1$ to N **do**
5.   Calculate interference on each user for all channel paths by neglecting the signal from the n-th antenna at time t.
6.   Multiply it with the Hermitian of the channel coefficient from n-th antenna to that user
7.   Sum the resulting terms for all users.
8.   Get the argument of the summation.
9. $\theta_n[t] = \pi + argument$
10.   **end for**
11.   **end for**
12. **end for**

Let $d_r \triangleq min(\tau, T - (r-1)\tau)$ and $L_r(t) = min(L-1, min(T, r\tau) - t)$ that is,

d_r represents the length of the block which is generally equal to τ except for the last block and it can be less than τ in the last one if T/τ is not integral. $L_r(t)$ addresses the channel length to be considered at time t which becomes less than L towards the end of the block since the signal received in the next block is not to be taken into consideration at the current one. Therefore, there are Nd_r subiterations in each iteration, and all the antenna phases are determined sequentially. After the (n, q)-th iteration where n represents the antenna index and q is for the time index, the algorithm moves to the $(n + 1, q)$-th iteration if $n < N$, and it moves to the $(1, q + 1)$-th iteration if $n = N$ and $q < d_r$. If the subiteration Nd_r is completed, then the algorithm moves to the next iteration. At the (n, q)-th subiteration, $Nd_r - 1$ phase angles are fixed and the (n, q)-th phase angle is calculated as follows

$$\begin{aligned}\theta_n[(r-1)\tau + q] &= \underset{\phi\in[-\pi,\pi)}{\operatorname{argmin}} f_r(\theta_1[(r-1)\tau + 1], ...\phi, ..., \theta_N[(r-1)\tau + d_r]) \\ &= \pi + arg\Bigg(\sum_{t=(r-1)\tau+q}^{(r-1)\tau+q+L_r((r-1)\tau+q)} \sum_{k=1}^{M} h^*_{k,n}[t-(r-1)\tau-q] S_{n,(r-1)\tau+q}(k,t)\Bigg)\end{aligned} \tag{2.23}$$

where

$$S_{n,(r-1)\tau+q}(k,t) \triangleq \frac{\sum_{i=1}^{N}\sum_{l=0,\,(i,l)\neq(n,t-(r-1)\tau+q)}^{L-1} h_{k,i}[l]e^{j\theta_i[t-l]}}{\sqrt{N}} - \sqrt{E_k}u_k[t].$$

At the (n, q)-th subiteration, the signal from the n-th antenna at time q is not used which is clearly shown by

$$S_{n,(r-1)\tau+q}(k,t) = \frac{\sum_{i=1}^{N}\sum_{l=0}^{L-1} h_{k,i}[l]e^{j\theta_i[t-l]}}{\sqrt{N}} - \sqrt{E_k}u_k[t] - \frac{h_{k,n}[t-(r-1)\tau+q]e^{j\theta_i[t-l]}}{\sqrt{N}}. \tag{2.24}$$

The complexity of computing NT transmit phase angles in Algorithm 2 is $O(NMLT)$ if $\tau \gg L$. Therefore, the complexity for per channel use becomes $O(NML)$.

2.4.2 Achievable Information Sum Rate

When the proposed CE precoding algorithm for frequency selective channels is employed, the phase angle transmitted from the n-th antenna at time t is calculated as $\hat{\theta}_n^u[t]$ for the scaled information symbol vectors, $\mathbf{u}[t], t = 1, ..., T$. Then, the MUI signal at the k-th user at time t is given by

$$I_k^u[t] = \frac{\sum_{i=1}^{N}\sum_{l=0}^{L-1} h_{k,i}[l]e^{j\hat{\theta}_i^u[t-l]}}{\sqrt{N}} - \sqrt{E_k}u_k[t]. \tag{2.25}$$

Thus, the received signal at the k-th user at time t is expressed in terms of the MUI energy as follows

$$y_k[t] = \sqrt{P_{BS}}\sqrt{E_k}u_k[t] + \sqrt{P_{BS}}I_k^u[t] + w_k[t] \tag{2.26}$$

where $w_k[t]$ is the additive white Gaussian noise term.

If $\mathbf{y_k} = [y_k[1], ..., y_k[T]]^T$ is the received signal vector, $\mathbf{u_k} = [\sqrt{E_k}u_k[1], ..., \sqrt{E_k}u_k[T]]^T$ is the scaled information symbol vector, $\mathbf{w_k} = [w_k[1], ..., w_k[T]]^T$ is the additive white Gaussian noise vector, $\mathbf{I_k^u} = [I_k^u[1], ..., I_k^u[T]]^T$ is the MUI energy vector at the k-th user, and $\mathbf{H}$ represents all channel vectors from the BS antennas to users, then the conditional mutual information between $\mathbf{y_k}$ and $\mathbf{u_k}$ becomes

$$I(\mathbf{y_k}; \mathbf{u_k}|\mathbf{H}) = h(\mathbf{u_k}) - h(\mathbf{u_k} - \frac{1}{\sqrt{P_{BS}}}\mathbf{y_k}|\mathbf{y_k}, \mathbf{H}) \tag{2.27}$$

Differential entropy is maximized for independent identically distributed (i.i.d) complex Gaussian random variables (under a power constraint). If $\mathbf{u_k}$ is selected as complex Gaussian, we obtain

$$I(\mathbf{y_k}; \mathbf{u_k}|\mathbf{H}) = Tlog_2(\pi e E_k) - h(\mathbf{u_k} - \frac{1}{\sqrt{P_{BS}}}\mathbf{y_k}|\mathbf{y_k}, \mathbf{H}). \tag{2.28}$$

Then, by removing the conditioning on $\mathbf{y_k}$, a lower bound on the mutual information is derived as follows

$$I(\mathbf{y_k}; \mathbf{u_k}|\mathbf{H}) \geq Tlog_2(\pi e E_k) - h(\mathbf{u_k} - \frac{1}{\sqrt{P_{BS}}}\mathbf{y_k}|\mathbf{H}). \tag{2.29}$$

If the autocorrelation matrix is $\mathbf{R_z} \triangleq \mathbb{E}[\mathbf{z_k}\mathbf{z_k}^H]$ for a random complex vector $\mathbf{z_k}$ then complex Gaussian distribution becomes the one which maximizes the differential entropy. Therefore, $h(\mathbf{u_k} - \mathbf{y_k}\frac{1}{\sqrt{P_{BS}}}|\mathbf{H}) \leq log_2((\pi e)^T|\mathbf{R_z}|)$. With this observation, an achievable rate is expressed as

$$R_k(\mathbf{H}, \mathbf{E}, \frac{P_{BS}}{\sigma^2}) \triangleq T\, max\left(0, log_2(E_k) - \frac{log_2\left(\left|\mathbb{E}[\mathbf{I_k^u}\mathbf{I_k^u}^H|\mathbf{H}] + \frac{\sigma^2}{P_{BS}}\mathbf{I}\right|\right)}{T}\right) \quad (2.30)$$

where $|.|$ denotes the determinant, and the expectation is computed over the data symbols conditioned on the channel gains. In other words, for a given channel matrix $\mathbf{H}$, we have

$$I(\mathbf{y_k}; \mathbf{u_k}|\mathbf{H}) \geq R_k(\mathbf{H}, \mathbf{E}, \frac{P_{BS}}{\sigma^2}).$$

In order to calculate the ergodic achievable rates, expectation of $R_k(\mathbf{H}, \mathbf{E}, \frac{P_{BS}}{\sigma^2})$ over the channel statistics is also needed.

As an example, we simulate the achievable information rate in bits per channel use versus the number of BS antennas for different number of users and channel lengths in Fig. 2.4. The channel paths are assumed to be independent Rayleigh fading $\sim CN(0, 1/L)$, and the codebooks are assumed to be complex Gaussian for all the users with $U_1 = U_2 = ... = U_M = CN(0, 1)$.

Observations from Fig. 2.4 are very similar to the corresponding results with the flat fading case (reported in Fig. 2.3). It is observed that when the symbol energy and the average BS power are fixed, increasing the number of BS antennas provides improvements in per user achievable information rate. Also, it is observed that after some point the MUI becomes negligible compared to AWGN power, hence increasing the number of antennas further does not offer any improvements in the resulting achievable information rates. Furthermore, when the channel length is small, the performance of the algorithm is improved because the dependence between consecutively received signals is reduced.

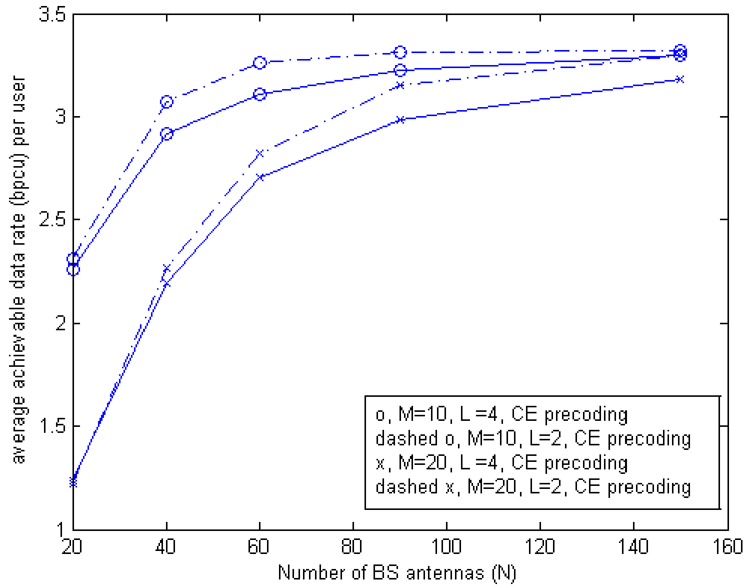

Figure 2.4: Average achievable data rate (in bpcu) versus the number of BS antennas. $P_{BS} = E_k = 1$, $\sigma^2 = 0.1$, $\tau = 3L$ and $T = 3\tau$.

2.5 Chapter Summary

In this chapter, we have reviewed two important subjects related to massive MIMO systems which will be used throughout the the thesis. Namely, we have discussed zero-forcing precoding and CE precoding solutions under both flat fading channels and frequency selective channels for massive MIMO systems [30, 31]. We have shown that the array gain and suppression of the MUI energy are still achieved even if constant envelope precoding is used. However, it is also noticed that some additional power is required to achieve an ergodic information sum rate compared to APC precoding. In other words there is some performance loss in the achievable rates and power efficiencies offered by CE precoding. The rest of the thesis addresses approaches trying to close this gap while still maintaining the benefits of CE precoding.

Chapter 3

Multi-Envelope Precoding for Massive MIMO Systems

As discussed in the previous chapter, constant envelope precoding is an effective method to obtain array gain and suppression of multi-user interference for massive MIMO systems under both flat fading and frequency selective fading conditions. However, the CE constraint is much more restrictive than the APC, hence it requires a higher power compared to APC precoding for the same achievable sum rate. For example, for a system with 200 antennas serving 10 mobile users over independent Rayleigh fading channels, for an achievable rate of 2 bits per channel use per user, 1.7 dB more power is needed as illustrated in Chapter 2.

With the objective of closing the performance gap between the CE precoding and the APC precoding solutions, in this chapter, we propose the use of more than one but only a few (e.g., 2 or 3) power amplifiers. To do this, we group the BS antennas, split the total power among these groups, and apply CE precoding to each group separately resulting in a multi-envelope precoding solution. We split the power before angle determination stage as shown in Fig. 3.1 to be able to use low complexity algorithms in [30, 31] as simultaneously determining the envelope levels and the phases increases the complexity of the system. We consider multi-envelope precoding solution for both flat fading and frequency selective fading channel conditions.

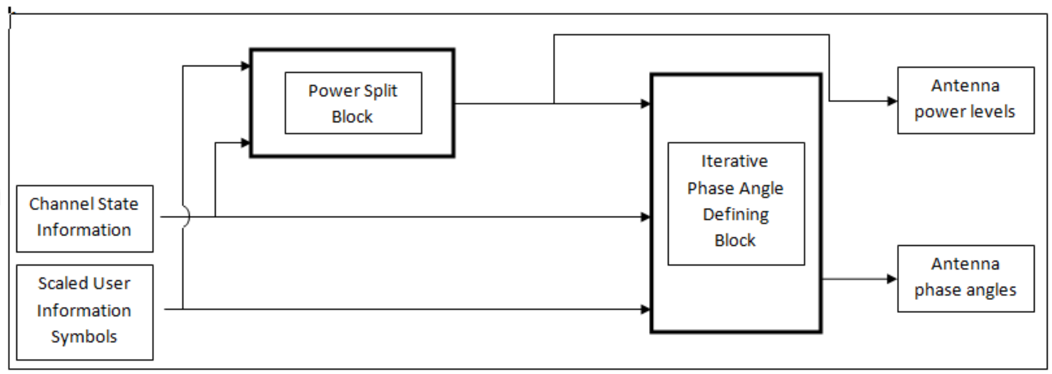

Figure 3.1: Multi-envelope precoding block diagram.

The chapter is organized as follows: we explain the proposed multi-envelope precoding approach in massive MIMO systems for flat fading channels and provide numerical examples that compare the new algorithm with the CE and APC precoding solutions in Section 3.1. We then modify the solution to the case of frequency selective fading in Section 3.2, and compare the multi-envelope precoding result with those of CE precoding via numerical examples. The chapter is concluded in Section 3.3.

3.1 Multi-Envelope Precoding over Flat Fading Channels

The system model is very similar to the one in Chapter 2, hence we do not repeat it here. The difference is in the solution approach, that is, here we have multiple groups of antennas with different envelope levels. For antenna grouping, we have considered different methods including use of the sum of the absolute values of the channel gains from an antenna element to all the users, however, the most effective technique is found to be using a zero-forcing precoding solution first and identifying the groups based on its results. This approach use both CSI and user symbol information in grouping the antennas.

Zero-forcing precoding is a successful method with the average only power constraint to cancel out the MUI energy, and hence it can work in interference free region [1]. Therefore, grouping the antennas by considering the zero-forcing criteria and supplying more power on the antennas that require higher signal levels have the potential to decrease the gap between the APC precoding and the CE precoding solutions.

3.1.1 Antenna Grouping by Zero-Forcing Precoder

We denote the power coefficient vector with $\mathbf{p}_{zf}^{N\times 1} = [p_{zf}^1, p_{zf}^2, ..., p_{zf}^N]^T$ where p_{zf}^n is power coefficient for the n-th antenna. With a PAs, the elements of $\mathbf{p}_{zf}$ take on a distinct values. We calculate the zero-forcing vector as in (2.2) and use the absolute value of its elements to generate $\mathbf{p}_{zf}$. Values of the power coefficients and the number of antenna elements in each group can be determined according to the PAs used at the BS circuitry. For simplicity, we assume that N is divisible by the number of PAs and we use groups of equal number of elements. Hence, we choose the power coefficient (envelope) of each group by considering the total BS power constraint, $\mathbf{p}_{zf}^T \mathbf{p}_{zf} = N$. As the number of elements in each group is equal, $\dfrac{p_1^2 + p_2^2 + ... + p_a^2}{a} = 1$. For instance, $p_1 > 1$ is considered as the coefficients of the first group of antennas (the corresponding absolute value of the term in the zero forcing vector is greater than that of the remaining half of the antennas) and $p_2 = \sqrt{2 - p_1^2}$ is the envelope level for the remaining ones if there are 2 PAs at the BS.

Then, the received signal at the k-th user is expressed as

$$y_k = \sqrt{P_{BS}/N} \sum_{n=1}^{N} h_{k,n} p_{zf}^n e^{j\theta_n} + w_k, k = 1, 2, ..., M. \tag{3.1}$$

If the information symbol of the k-th user u_k is used in (3.1), the received signal is expressed as

$$y_k = \sqrt{P_{BS}} \sqrt{E_k} u_k + \sqrt{P_{BS}} s_k + w_k, \tag{3.2}$$

where

$$s_k = \frac{1}{\sqrt{N}} \sum_{n=1}^{N} h_{k,n} p_{zf}^n e^{j\theta_n} - \sqrt{E_k} u_k \tag{3.3}$$

is the MUI term at the k-th user.

3.1.2 Precoder Design

Signal envelopes are determined before the phase angle solution stage. In order to solve the transmission phase angles resulting in small MUI energies compared to the complex Gaussian noise at each user, a nonlinear least squares optimization problem in (3.4) is formulated for known $\mathbf{u}$, CSI and $\mathbf{p}_{zf}$ values, namely,

$$\begin{aligned}\boldsymbol{\theta}^u = [\theta_1^u, ..., \theta_N^u] &= \underset{\theta_i \in [-\pi,\pi), i=1,...,N}{\operatorname{argmin}} g(\boldsymbol{\theta}, \mathbf{u}), \\ g(\boldsymbol{\theta}, \mathbf{u}) \triangleq \sum_{k=1}^{M} |s_k|^2 &= \sum_{k=1}^{M} \left| \frac{\sum_{n=1}^{N} h_k^n p_{zf}^n e^{j\theta_n}}{\sqrt{N}} - \sqrt{E_k} u_k \right|^2\end{aligned} \tag{3.4}$$

As in the solution of CE precoding reviewed in Chapter 2, the solution of this optimization problem at most local minima is small enough if the ratio of N/M is high. Therefore, Algorithm 1 of Chapter 2 can be modified as Algorithm 3 to calculate the transmission phase angles for a given $\mathbf{p}_{zf}$ vector.

In Algorithm 3, iterations proceed in the same way as in Algorithm 1, however, the function for determining the phase angles changes as antennas have different power coefficients instead of the same envelope levels. At the $(p, q+1)$-th iteration, $\boldsymbol{\theta}^{p,q+1}$ is calculated by using

$$\begin{aligned}\boldsymbol{\theta}^{(p,q+1)} &= \underset{\boldsymbol{\theta}=\theta_1^{(p,q)},...\theta_q^{(p,q)},\phi,\theta_{q+2}^{(p,q)},...,\theta_N^{(p,q)},\phi\in[-\pi,\pi)}{\operatorname{argmin}} g(\boldsymbol{\theta}, \mathbf{u}), \\ &= \pi + arg\left(\sum_{k=1}^{M} \frac{h_{k,q+1}^*}{\sqrt{N}} \left[\left(\frac{1}{\sqrt{N}} \sum_{n=1,\neq q+1}^{N} h_{k,n} p_{zf}^n e^{j\theta_n^{(p,q)}} \right) - \sqrt{E_k} u_k \right] \right) \\ \theta_i^{(p,q+1)} &= \theta_i^{(p,q)}, i = 1, 2, ..., N, i \neq q+1.\end{aligned} \tag{3.5}$$

while all other phase angles are kept the same with the previous sub-iteration.

In Algorithm 3, there are two serial stages: determination of the power coefficient vector and solving the transmission phase angles for a given power coefficient vector to minimize the objective function. In the first part, calculation of the zero forcing vector includes pseudo inverse calculation of an $N \times M$ matrix which has complexity $O(M^2N)$, and matrix vector product whose complexity is $O(MN)$. The second part of the algorithm has the same complexity as the Algorithm 1, (i.e., $O(MN)$). Therefore, Algorithm 3 has an overall complexity in the order of $O(M^2N)$ which is slightly higher than that of Algorithm 1.

Algorithm 3 Proposed iterative multi-envelope precoding algorithm for massive MIMO systems.

1. Calculate zero-forcing vector, $\mathbf{v}_{zf} = [v^1_{zf}, v^2_{zf}, ..., v^N_{zf}]^T$ as in 2.2.
2. Calculate power coefficient vector $\mathbf{p}_{zf}$ by using $\mathbf{v}_{abs} = [|v^1_{zf}|, |v^2_{zf}|, ..., |v^N_{zf}|]^T$.
3. $\boldsymbol{\theta} = \mathbf{0}$
4. **for** $iter = 1$ to $iterationCount$ **do**
5. **for** $i = 1$ to N **do**
6. Calculate interference on each user by neglecting the signal from the i-th antenna
7. Multiply interference value with the conjugate of the channel from i-th antenna to the user.
8. Sum the resulting terms for all users.
9. Get the argument of the summation.
10. $\theta_i = \pi + argument\, found\, above$
11. **end for**
12. **end for**

Denoting the phase angles after the last iteration as $\hat{\boldsymbol{\theta}}^u = [\hat{\theta_1}^u, ..., \hat{\theta_N}^u]^T$, the MUI signal at the k-th user is given by

$$\hat{s}_k = \left(\frac{\sum_{n=1}^{N} h_{k,n} p_{zf}^n e^{j\hat{\theta}_n^u}}{\sqrt{N}} - \sqrt{E_k} u_k \right). \tag{3.6}$$

Then, the SINR expression can be computed from (2.12) by using this MUI signal, and employing the lower bound to the mutual information in (2.16), the achievable rate is obtained as in (2.17) similar to the case of CE precoding.

3.1.3 Examples

In this part, we provide example designs and simulate their performance.

Two-Envelope Precoding

With the use of two PAs at the BS, the power coefficient vector includes only two different values denoted by p_1 and p_2 where $p_1^2 + p_2^2 = 2$, i.e., $p_2 = \sqrt{2 - p_1^2}$, if the number of antennas fed by both of the PAs are equal. Then, the zero-forcing vector is calculated using (2.2) and the vector of the absolute values of its elements is used to determine the antennas which will be assigned to the first envelope. That is, antennas whose corresponding value in the absolute value of the zero forcing vector are greater are chosen for the larger envelope and the others for the smaller envelope level. After this separation, there will be two groups with $N/2$ antennas each. The CE precoding is applied to these groups individually to obtain the two-envelope solution. Nonlinear amplifiers can still be used in this case since the constant gain regions with levels (p_1 and p_2) of the PAs are utilized.

The scheme is illustrated in Fig. 3.2. Each PA has connection to all the antennas, however, through the RF switch block one PA feeds $N/2$ antennas at any given time interval. Then, the corresponding phases of the signals of all the antennas are applied

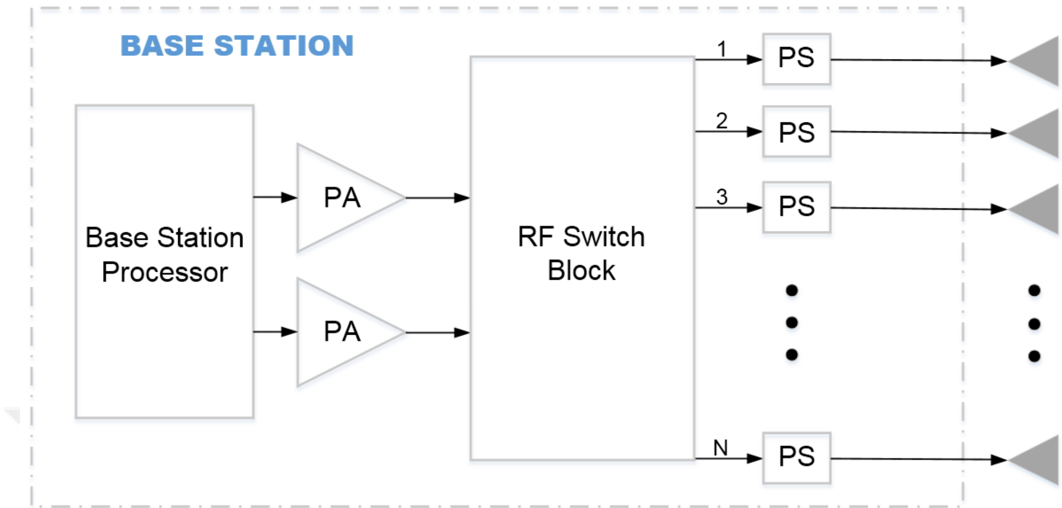

Figure 3.2: BS RF chain with 2 PAs

via phase shifters, and the resulting two-envelope precoded signal is transmitted.

We illustrate the resulting performance for the proposed two-envelope precoding (for the same set-up as in Fig. 2.1) in Fig 3.3. The power levels are selected as $p_1 = \sqrt{3/2}$ and $p_2 = \sqrt{1/2}$.

It is observed that the MUI energy with two-envelope precoding is always less than the one with the CE precoding. This shows that the two-envelope precoding with antenna grouping by the zero-forcing algorithm promises to decrease the required BS power to provide the same achievable information rate with the CE precoding solution, i.e., the same SINR performance can be achieved with a smaller transmission power. Another way to interpret this result is that a smaller number of BS antennas (e.g., 72 versus 80) are needed for the same MUI level.

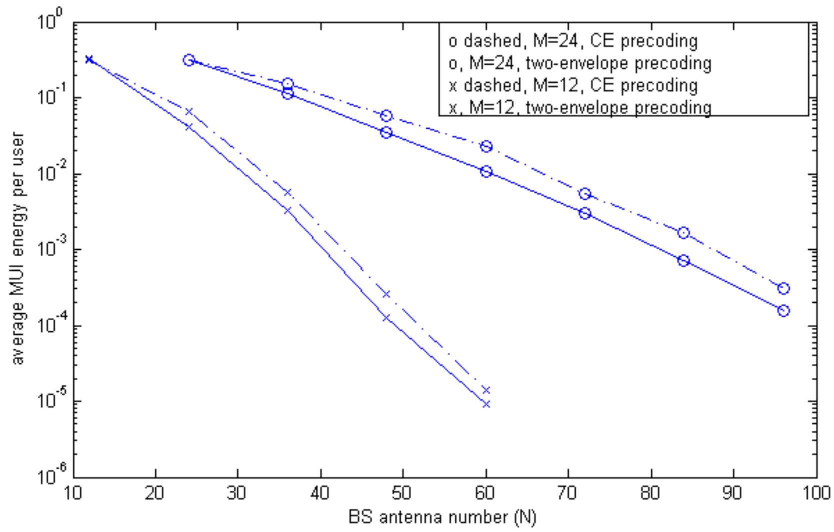

Figure 3.3: Average per-user MUI energy versus the number of BS antennas. $p_1 = \sqrt{3/2}$, Rayleigh fading.

The value of p_1 needs to be optimized further, in order to minimize the required BS power. However, the function $g(\boldsymbol{\theta}, \mathbf{u})$ is hard to analyze theoretically. Hence, we try different power coefficients and observe the behavior of the average MUI in Fig. 3.4 numerically.

The results are encouraging in the sense that it is not necessary to optimize the power levels with a high accuracy as $p_1 = \sqrt{3/2}$, $p_1 = \sqrt{5/3}$, $p_1 = \sqrt{7/4}$ have shown similar performances. However, $p_1 = \sqrt{15/8}$ has caused an increase in MUI energy which is reasonable because diversity gain caused by the half of the antennas decreases as p_1 approaches to 2 too closely. We choose $p_1 = \sqrt{3/2}$ as the power coefficient which will be used in further simulations.

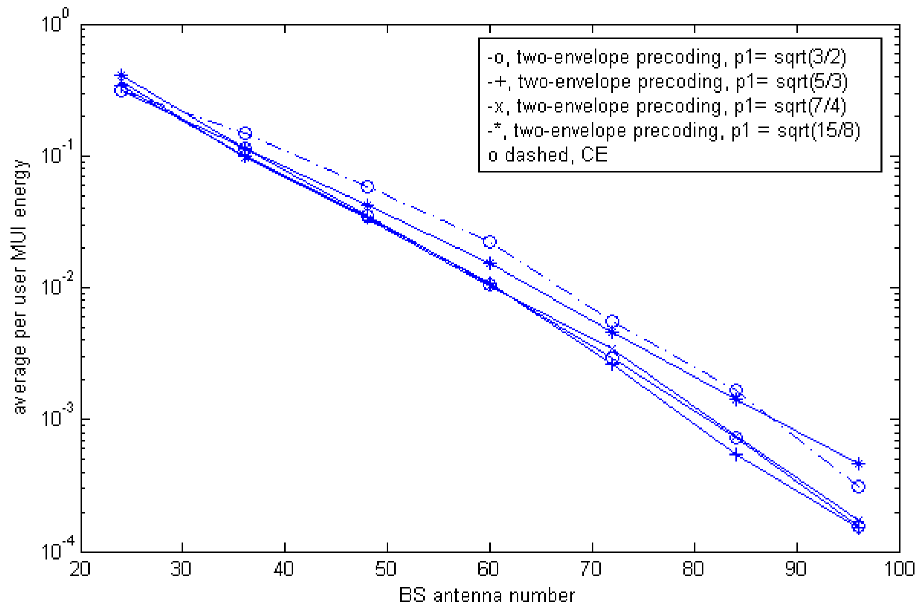

Figure 3.4: Average per-user MUI energy versus the number of BS antennas for varying envelope levels. $M = 24$, Rayleigh fading.

We further utilize different grouping strategies to observe the behavior of the per user MUI energy in Fig. 3.5. With $p_1 = \sqrt{3/2}$, we select 40%, 30%, and 20% of the antennas for the first group, respectively and apply the same precoding algorithm in addition to the case of equal size groups. From the numerical results, we observe that equal size grouping provide slightly better performance than the other grouping strategies.

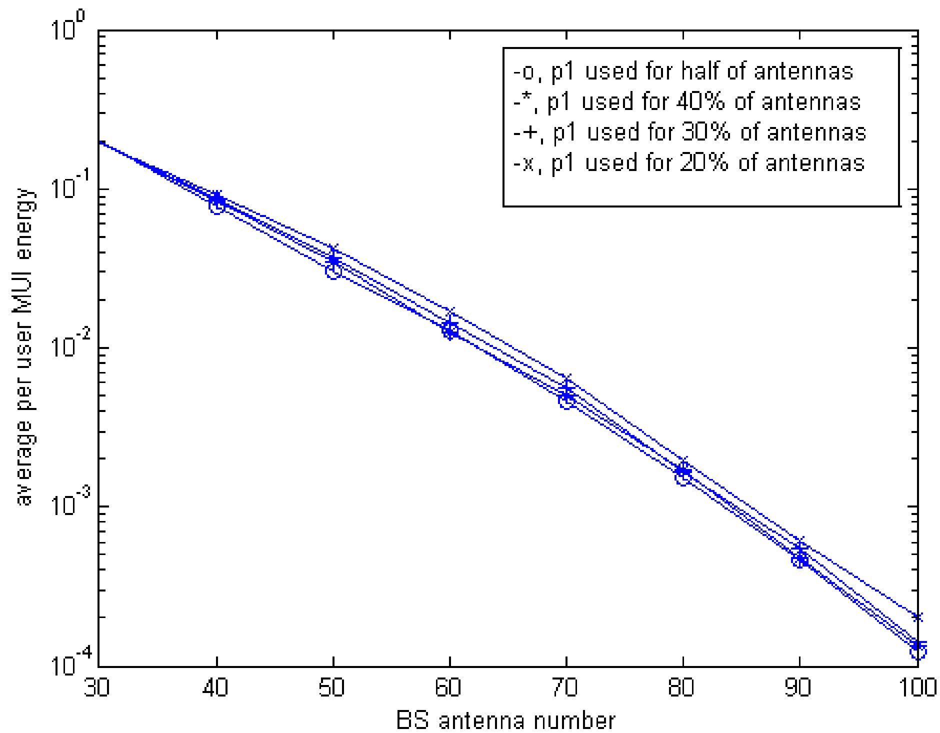

Figure 3.5: Average per-user MUI energy versus the number of BS antennas for different grouping strategies. $M = 24$, Rayleigh fading.

Three-Envelope Precoding

If three PAs are utilized at the BS, $\mathbf{p}_{zf}$ includes three different values denoted by p_1, p_2 and p_3. The first group of antennas which correspond to elements with highest absolute values in the zero-forcing vector have the greatest envelope levels. The second one includes antennas with the second highest absolute values and so on.

We note that the RF chain in the first example (Fig. 3.2) is also valid for this set-up, however, the number of PAs which are connected to the antennas is three.

We simulate the MUI for the three-envelope case and compare it with two-envelope precoding and CE precoding solutions in Fig. 3.6. We use $p_2 = 1$, $p_3 = \sqrt{1/2}$ and $p_1 = \sqrt{2 - p_3^2} = \sqrt{3/2}$ as the power coefficients. We split the antennas equally to three of the groups by assuming that $N/3$ is integral without loss of generality, however, different designs are also possible. The set-up is the same as the one in Fig. 3.3.

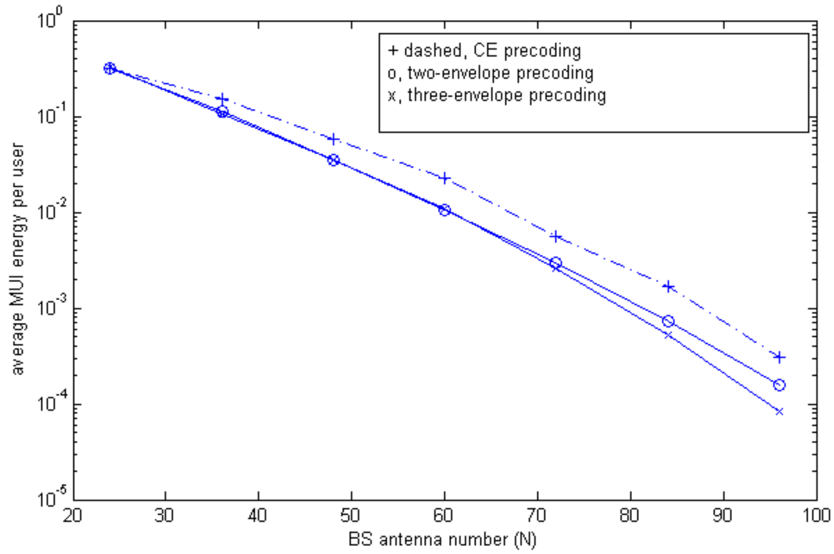

Figure 3.6: Average per-user MUI energy versus the number of BS antennas. $M = 24$, Rayleigh fading.

We observe that the three-envelope precoding offers slightly better performance than the two-envelope precoding solution which is expected since it is closer to the APC precoding as the zero-forcing criteria is used to group antennas and more envelope levels are available.

In Fig. 3.7, we use different sets of coefficients in three-envelope precoding to observe the behavior of the objective function in (3.4) (which is hard to analyze analytically). We keep $p_2 = 1$ and change p_1 and p_3 while keeping the total power requirement satisfied. That is, we choose $p_1 = \sqrt{2 - p_3^2}$.

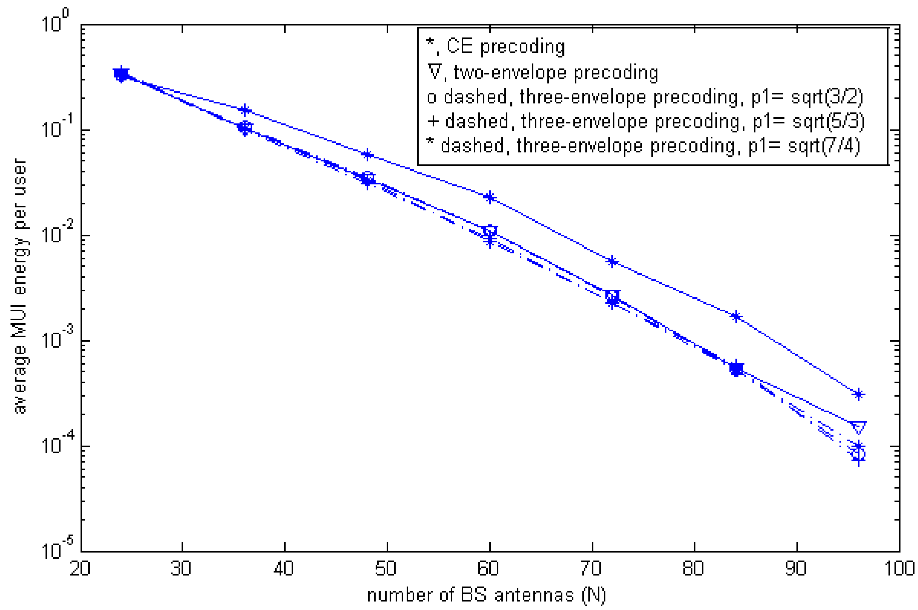

Figure 3.7: Average per-user MUI energy versus the number of BS antennas for varying envelope levels. $M = 24$, Rayleigh fading.

We observe that there is no significant improvement with the change of p_3 among the values $\sqrt{1/2}$, $\sqrt{1/3}$ and $\sqrt{1/4}$. Therefore, we choose $p_3 = \sqrt{1/2}$ for use in the rest of the examples.

After studying the MUI energy with two and three envelope precoding, we simulate the required power for a certain achievable rate for CE and multi-envelope precoding techniques by conducting similar simulations as in Fig. 2.2. We utilize the same power coefficients as in the earlier examples, i.e., $p_1 = \sqrt{3/2}$ and $p_2 = \sqrt{1/2}$ for two-envelope precoding, and $p_1 = \sqrt{3/2}$, $p_2 = 1$ and $p_3 = \sqrt{1/2}$ for the three-envelope precoding.

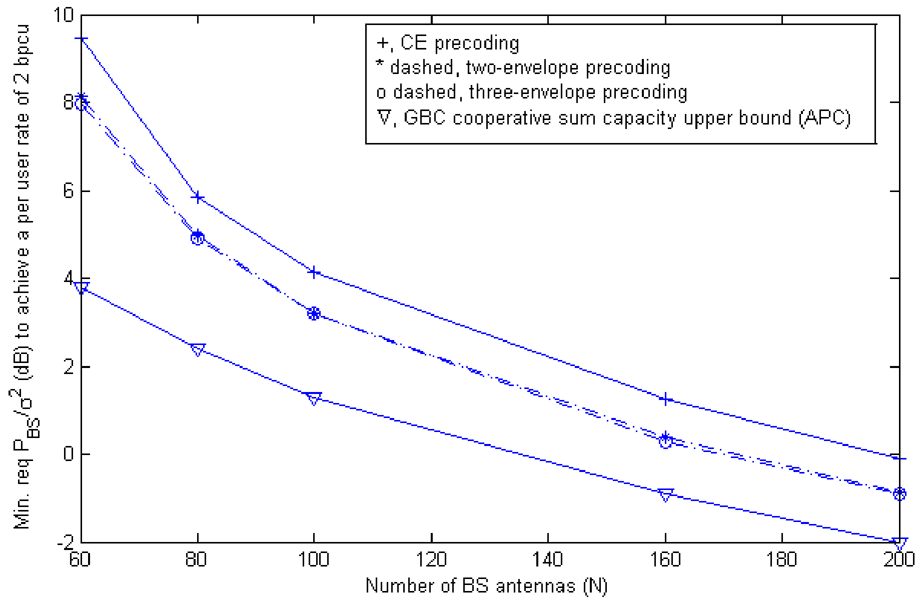

Figure 3.8: The required $\dfrac{P_{BS}}{\sigma^2}$ ratio versus the number of antennas. $M = 40$, Rayleigh fading.

In order to show the resulting improvement with multi-envelope precoding compared to the CE precoding solution, cooperative upper bound on the GBC sum-capacity is also plotted [30, 38]. From Fig. 3.8, we observe that the extra power required by utilizing the CE constraint decreases with the use of 2 and 3 PAs and antenna grouping according to presented zero-forcing algorithm. For example, for $N = 160$, this gain is around 1 dB. Further, it is demonstrated that there is no significant difference between 2 or 3 envelope levels.

3.2 Multi-Envelope Precoding for Massive MIMO Systems over Frequency Selective Channels

We further explore the multi-envelope precoding idea which decreases the power requirements for a given achievable rate in massive MIMO systems for flat fading channels to the case of frequency selective fading. For this purpose, we modify the zero-forcing algorithm for antenna grouping and split the total power among these groups.

3.2.1 Antenna Grouping by Using the Zero Forcing Vector

The system model is very similar to the one in Chapter 2. As it is explained in Section 2.4, for frequency selective channels there is ISI among the received symbols necessitating a modification of the iterative algorithm which solves for the phase angles in CE precoding. The presence of ISI also affects the methodology of antenna grouping with the use of zero-forcing algorithm, that is the ISI term has to be taken into account in the modification of the algorithm.

Realistic channel models are casual, hence the received signal at the current time is only a function of the current and the previous transmissions. Transmission in the previous time instances are known at the BS while calculating the signals for the current time. Therefore, we subtract the effect of the previous transmissions and determine the zero-forcing vector for the remaining signal as summarized in Algorithm 4. We denote the power coefficient vector at time t with $\mathbf{p}_{zf}[t] = [p^1_{zf}[t], p^2_{zf}[t], ..., p^N_{zf}[t]]^T$ and power coefficient matrix for all the antennas and entire channel coherence time as $\mathbf{P}^{NT}_{zf} = [\mathbf{p}_{zf}[1]\,\mathbf{p}_{zf}[2]\,...\,\mathbf{p}_{zf}[T]]$. As in the multi-envelope precoding over flat fading channels, the number of different values in $\mathbf{P}_{zf}$ depends on the number of PAs at BS and all the PAs are connected to all the BS antennas, however, they feed a predetermined group of them at a time (Fig. 3.2).

Algorithm 4 Power coefficient matrix determination by utilizing the absolute value of the elements of zero-forcing vector for massive MIMO systems over frequency selective channel.

1. **for** $t = 1$ to T **do**
2. $\mathbf{m} = \mathbf{u}[t]$
3. **for** $i = 2$ to $min(t, channelLength)$ **do**
4. Subtract ISI signals from the channel path, $i-1$, $\mathbf{m} = \mathbf{m} - \mathbf{H}_{i-1}\mathbf{s}_{i-1}$ where $\mathbf{s}_{i-1}$ denotes for transmitted signal at time $t - i + 1$
5. **end for**
6. Calculate the pseudo inverse of the shortest path of the channel matrix $(\mathbf{H_0})$, $\mathbf{H}_{si} = \mathbf{H_0}'(\mathbf{H_0}\mathbf{H_0}')^{-1}$
7. Calculate the zero forcing vector for the effective required signal vector, $\mathbf{v}_{zf} = \mathbf{H}_{si}\mathbf{m}$
8. Determine $\mathbf{p}_{zf}[t]$ by using $\mathbf{v}_{abs} = [|v_{zf}^1|, |v_{zf}^2|, ..., |v_{zf}^N|]^T$.
9. **end for**

As in Fig. 3.2, $\mathbf{P}_{zf}$ is calculated before solving for the phase angles. Therefore, the ISI signal subtraction in Algorithm 4 is done by assuming that the transmitted signals are calculated with the zero-forcing precoding approach, clearly, this is not optimal. However, we will later see that it is effective.

Following the notation in Section 2.4 and denoting $p^n_{zf}[t]$ for the n-th component of $\mathbf{P}_{zf}$ at time t, the received signal at the k-th user is given by

$$y_k[t] = \sqrt{\frac{P_{BS}}{N}} \sum_{n=1}^{N} \sum_{l=0}^{L-1} h_{k,n}[l] p^n_{zf}[t-l] e^{j\theta_n[t-l]} + w_k[t], \tag{3.7}$$

where $w_k[t]$ is circularly symmetric complex Gaussian noise.

3.2.2 Precoder Design

With a given set of user symbols for entire coherence time, $\mathbf{u}[1], \mathbf{u}[2], ..., \mathbf{u}[T]$, the CSI, and the power coefficient matrix $\mathbf{P}_{zf}$, the optimization problem below is formulated to determine the phase angles to be transmitted as

$$\begin{aligned}
&[\mathbf{\Theta}^u[1], \mathbf{\Theta}^u[2], ..., \mathbf{\Theta}^u[T]] = \underset{\theta^u_{n,t} \in [-\pi,\pi), t=1,2,...,T, n=1,2,...,N}{\operatorname{argmin}} \sum_{r=1}^{\lceil T/r \rceil} I_r \\
&I_r \triangleq f(\Theta[(r-1)T - L + 2], ..., \Theta[min(T, r\tau)], \mathbf{u}[(r-1)T + 1], ..., \mathbf{u}[min(T, r\tau)]) \\
&= \sum_{t=(r-1)\tau+1}^{min(T,r\tau)} \sum_{k=1}^{M} \left| \frac{\sum_{n=1}^{N} \sum_{l=0}^{L-1} h_{k,n}[l] p^n_{zf}[t-l] e^{j\theta_n[t-l]}}{\sqrt{N}} - \sqrt{E_k} u_k[t] \right|^2 .
\end{aligned} \tag{3.8}$$

As it is explained in Section 2.4, the phase angle optimization problem is done over multiple shorter blocks due to the excess number of optimization variables. Algorithm 2 is also valid for this problem except for the use of power coefficients in the optimization process and the angle calculation equations. In other words, the iterative procedure and the solution approach for determining the angles are the same as those in Algorithm 2. The difference is that the specific angle calculation step is given by

$$\theta_n[(r-1)\tau+q] = \underset{\phi\in[-\pi,\pi)}{\operatorname{argmin}} f_r(\theta_1[(r-1)\tau+1], ..., \phi, ..., \theta_N[(r-1)\tau+d_r])$$
$$= \pi + arg\Bigg(\sum_{t=(r-1)\tau+q}^{(r-1)\tau+q+L_r((r-1)\tau+q)} \sum_{k=1}^{M} h^*_{k,n}[t-(r-1)\tau+q]S_{n,(r-1)\tau+q}(k,t)\Bigg) \tag{3.9}$$

where

$$S_{n,(r-1)\tau+q}(k,t) \triangleq \frac{\sum_{i=1}^{N}\sum_{l=0,\,(i,l)\neq(n,t-(r-1)\tau+q)}^{L-1} h_{k,i}[l]p^i_{zf}[t-l]e^j\theta_i[t-l]}{\sqrt{N}} - \sqrt{E_k}u_k[t].$$

Denoting $\hat{\theta}^u_n[t]$ as the phase angle at the n-th antenna at time t, the MUI term at the k-th terminal at time t is given by

$$I^u_k[t] = \frac{\sum_{i=1}^{N}\sum_{l=0}^{L-1} h_{k,i}[l]p^i_{zf}[t-l]e^{j\hat{\theta}^u_i[t-l]}}{\sqrt{N}} - \sqrt{E_k}u_k[t]. \tag{3.10}$$

By using the MUI term in (3.10), a lower bound to mutual information, and hence, an achievable rate is calculated using (2.29) and (2.30).

Antenna grouping and optimization of phase angles are two serial stages where calculation of transmit phase values to minimize the objective function requires the knowledge of the power coefficient matrix. Calculation of the power coefficient matrix as in Algorithm 4 requires pseudo inverse calculation of an $N \times M$ matrix for the entire coherence time resulting in a complexity in the order of $O(M^2NT)$, and matrix vector product whose complexity is $O(MNLT)$. The phase angle determination part has the same complexity with Algorithm 2 which is $O(MNLT)$. Therefore, the multi-envelope precoding for massive MIMO systems over frequency selective channels has an overall complexity of $O(M^2NT)$ as $M > L$, hence it is slightly worse the one with the CE precoding in Algorithm 2.

3.2.3 Examples

We now simulate the achievable information rate of CE precoding and multi-envelope precoding for massive MIMO systems over frequency selective channels. We consider a four equal power channel with independent $CN(0, 1/L)$ channel taps i.e., each tap is Rayleigh fading. Block length, $\tau = 3L$ and coherence time of the channel is 3τ. For multi-envelope precoding, 2 PAs are utilized at the BS. As in the flat fading case, one PA feeds half of the antennas. Therefore, the power coefficients are determined as $p_1 = \sqrt{2 - p_2^2}$ to satisfy total power constraints.

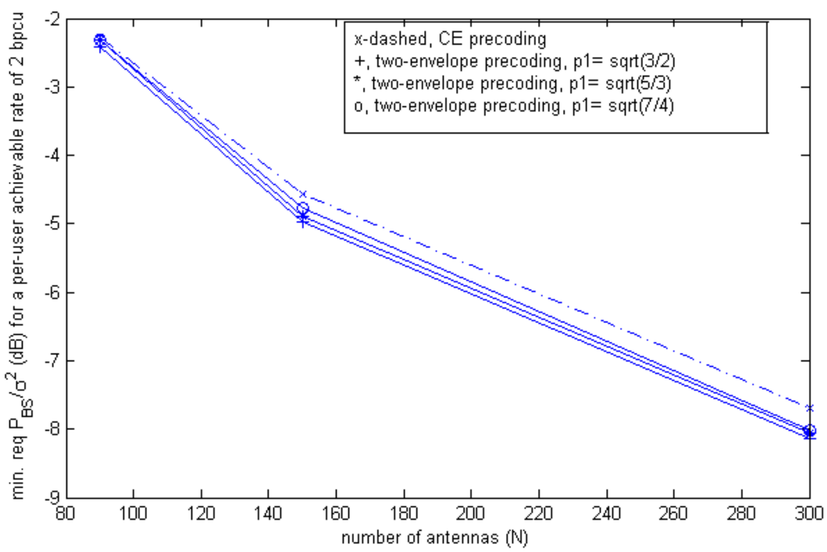

Figure 3.9: The required $\dfrac{P_{BS}}{\sigma^2}$ ratio versus the number of BS antennas for $M = 10$ users.

Table 3.1: Minimum required P_{BS}/σ^2 (dB) for a given ergodic achievable rate of 2 bpcu.

	N=20	**N=40**	**N=90**	**N=150**	**N=300**
CE precoding	7.19 dB	2.15 dB	-2.28 dB	-4.58 dB	-7.69 dB
Multi Envelope Level Precoding $p_{zf} = \sqrt{1/2}$	6.88 dB	1.89 dB	-2.42 dB	-4.97 dB	-8.13 dB
Multi Envelope Level Precoding $p_{zf} = \sqrt{1/3}$	6.95 dB	1.95 dB	-2.32 dB	-4.88 dB	-8.06 dB
Multi Envelope Level Precoding $p_{zf} = \sqrt{1/4}$	7.01 dB	2.03 dB	-2.31 dB	-4.77 dB	-8.02 dB

We consider different power coefficients including $\sqrt{1/2}$, $\sqrt{1/3}$, and $\sqrt{1/4}$ for p_2 to explore the behavior of the objective function which is hard to analyze theoretically. In Fig. 3.9, we observed that the proposed multi-envelope precoding decreases the performance loss even with the use of two PAs at the BS. This observation is clearer in Table 3.1. For instance, a gain of around 0.4 dB for the number of antennas in the order of 100-300 is obtained. Also, we observe that the required power for achieving a given rate decreases with increasing number of antennas and massive MIMO gain is satisfied by both algorithms, that is, by doubling the BS antennas necessary power decreases around 3 dB.

3.3 Chapter Summary

In this chapter, we have presented two multi-envelope precoding techniques for massive MIMO systems: one for flat fading channels and the other for frequency selective fading conditions. The solution is based on the idea of grouping antennas and utilizing different envelopes for each group. In order to group the antennas and split the total available power more efficiently, we have applied the zero-forcing precoding algorithm and we modified the algorithms in [30, 31] to solve for the phase angles by considering the introduced power coefficients. We have shown through simulations that the proposed multi-envelope precoding techniques are effective. For example, for the case of 200 BS antennas serving 40 mobile users over a flat fading channel, with the use of two PAs, the required power for an achievable rate of 2 bpcu decreases around 1 dB compared to the case of CE precoding. We conclude that the proposed multi-envelope precoding solutions perform better than the CE precoding and help to close the gap between APC precoding and CE precoding performances by utilizing only two or three PAs.

Chapter 4

Multi-Envelope Precoding with Digital Phase Shifters for Massive MIMO Systems

In the previous two chapters, the use of continuous phase shifters in precoding is considered, however, working with digital phase shifters which support a discrete set of phase values has many advantages including immunity to noise on voltage control signal, more uniform input-output performance and flat phase values over wider bandwidths [36]. As shown in [32], the use of discrete-phase shifters for massive MIMO systems for CE precoding results in a nonlinear discrete optimization problem. These kinds of problems typically have NP-hard (non-deterministic polynomial-time hard) complexity, and sub-optimal but highly efficient algorithms are necessary to obtain solutions in a reasonable time.

In [32], discrete-phase constant envelope precoding for massive MIMO systems is considered, and an approach called trellis based constant envelope precoding (TB-CEP) is proposed. In this chapter, we first review its results, and then we extend the approach taken to the case of multi-envelope precoding. We also provide numerical examples which compare multi-envelope precoding with discrete phase shifters with TB-CEP and CE precoding algorithms, and draw some conclusions.

4.1 Discrete-Phase Constant Envelope Precoding for Massive MIMO Systems

4.1.1 System Model

The system model is very similar to the one in Chapter 2. The received signal of the k-th user is expressed as

$$y_k = \sqrt{\frac{P_{BS}}{N}} \mathbf{h}_k \mathbf{q} + w_k \tag{4.1}$$

where $\mathbf{h}_k$ is channel vector to the k-th user, i.e., the k-th row of $\mathbf{H}$, $\mathbf{q} \triangleq [e^{j\theta_1}, e^{j\theta_2}, .., e^{j\theta_N}]^T$ is the phase vector, and w_k is zero mean complex circularly symmetric Gaussian noise with variance σ_w^2.

4.1.2 Problem Description

The received signal of the k-th user in (4.1) is expressed in terms of the desired signal $\sqrt{E_k} u_k$ as follows

$$y_k = \sqrt{E_k} u_k + \left(\sqrt{\frac{P_{BS}}{N}} \mathbf{h}_k \mathbf{q} - \sqrt{E_k} u_k \right) + w_k. \tag{4.2}$$

Here, $\left(\sqrt{\frac{P_{BS}}{N}}\mathbf{h}_k\mathbf{q} - \sqrt{E_k}u_k\right)$ is the MUI term. We need to reduce the sum of the MUI energies at each user in order to increase the achievable data rates. Therefore, the following nonlinear discrete optimization problem is formulated in [32]:

$$\begin{gathered}\hat{\mathbf{q}} = \underset{\mathbf{q}}{\operatorname{argmin}} \sum_{k=1}^{M} \left| \sqrt{\frac{P_{BS}}{N}}\mathbf{h}_k\mathbf{q} - \sqrt{E_k}u_k \right|^2, \\ s.t.\ q_n \in Q_m, n = 1, 2, ..., N,\end{gathered} \tag{4.3}$$

where Q_m is set of phase values supported by the phase shifters assumed to be $q_n = exp\left(j\frac{2\pi m_n}{m}\right)$ for $m_n \in \{0, 1, ..., m-1\}$. These kinds of integer programming problems have exponential complexity in the worst case. Therefore, solving the optimization problem in (4.3) by utilizing conventional methods is not suitable for massive MIMO systems where N is high. With this motivation, the problem is transformed into a new one by expanding the square in (4.3) and ignoring the terms which do not depend on $\mathbf{q}$ resulting in

$$\begin{gathered}\hat{\mathbf{q}} = \underset{\mathbf{q}}{\operatorname{argmin}} \sum_{j=1}^{N} Re\left(\sqrt{\frac{P_{BS}}{N}} \sum_{i=1}^{j-1} q_j^* \mathbf{G}_{j,i} q_i - \mathbf{u}^H \mathbf{E} \mathbf{h}_j q_j\right) \\ s.t.\ q_n \in Q_m, n = 1, 2, ..., N.\end{gathered} \tag{4.4}$$

where $\mathbf{G} = \mathbf{H}^H\mathbf{H}$, $\mathbf{h}_j$ is the j-th column of channel matrix, and the diagonal matrix $\mathbf{E}^{M\times M}$ includes the user symbol energies. The objective function in (4.4) has N real terms where the j^{th} term depends only on the first j variables.

By using the same methodology in [30], it is proven that interference on users becomes small enough compared to AWGN as N goes to infinity. Briefly, if the noise term is neglected, the number of possible received signal vectors at users is m^N, hence the received signal space becomes denser with increasing N since the transmission power is constant. Therefore, the probability of having a vector which provides a MUI energy less than any nonzero value increases and it is shown that this probability is in fact strictly greater than zero [32].

4.1.3 Trellis Based Constant Envelope Precoding

Thanks to the formation of the objective function in (4.4), that is, since the j^{th} term depends only on the first j variables, the problem is solvable with a multi-stage approach. Based on this observation, a greedy approach which determines the j^{th} phase value to minimize the objective function at this stage is considered as a proper method. However, considering the last few phase values as states and keeping the most likely paths for each state at the each stage until the last antenna taken into account and deciding all of the phases together is observed to be a better approach as it enhances the set of angles utilized for minimization of the objective function, hence a TB-CEP algorithm (similar to Viterbi algorithm) is devised.

As it is summarized in Algorithm 5, firstly the initial states are determined as all the possibilities of the phase values that are available with the utilized digital phase shifters. Thus, m^L initial states are created for a memory length of L. Then, the cumulative metrics are calculated for all the initial states as follows

$$\sum_{j=1}^{L} Re\left(\sqrt{\frac{P_{BS}}{N}}\sum_{i=1}^{j-1} q_j^* \mathbf{G}_{j,i} q_i - \mathbf{u}^H \mathbf{E} \mathbf{h}_j q_j\right). \tag{4.5}$$

We note that m branches go out of each state and m branches enter each state at each step. A state is determined by the latest $L-1$ phase values of the originating state and the branch label which is the phase chosen for the current stage. At the t-th stage, the branch metric is determined as follows

$$Re\left(\sqrt{\frac{P_{BS}}{N}}\sum_{i=1}^{t+L-1} q_{t+L}^* \mathbf{G}_{t+L,i} q_i - \mathbf{u}^H \mathbf{E} \mathbf{h}_{t+L} q_{t+L}\right). \tag{4.6}$$

The path with the least cumulative metric among the m branches which enter a state is chosen as the originating path and the others are discarded. The algorithm continues until the last antenna is accounted for, and the best path which provides the least objective value is chosen and the phase values are determined as the branch labels and the initial states of this path.

Algorithm 5 Trellis- based constant envelope precoding (TB-CEP) algorithm.

1. Create m^L initial states which are all possibilities of the possessed phase values.
2. For the initial states calculate metrics by using (4.5).
3. **for** $j = L + 1$ to N **do**
4. Calculate each branch metric by using the label values and the originating path values as in (4.6)
5. Calculate the cumulative metric for each branch by adding the originating state metric to the branch metric
6. Choose the branch with the least cumulative metric as the survival one
7. Set the state metric as the cumulative metric of the survival branch
8. **end for**
9. Choose the path with the least cumulative metric
10. Determine the antenna phases as the initial state values and the branch labels

There are $N - L$ stages and m^L states where m branches enter each state and the branch metrics are calculated by using (4.6). Therefore, the complexity of the algorithm is polynomial, i.e., $O(N^2 M m^{L+1})$ for each channel use [32].

After determination of the transmission phase, achievable rate for the k-th user is expressed as

$$R_k(\mathbf{q}) = log_2 \left(\frac{E_k}{I_k(\mathbf{q}) + \sigma_w^2} \right) \tag{4.7}$$

where $I_k(\mathbf{q})$ is MUI energy at the k-th user.

4.1.4 Examples

We now simulate the achievable information rate in bits per channel use versus the number of BS antennas for different discrete phase shifters in Fig. 4.1. The channels between the BS antennas and the mobile terminals are i.i.d. Rayleigh fading $\sim CN(0, 1)$, and $P_{BS} = E_k = 10$ for $k = 1, 2, ..., 10$ is used to avoid further optimization of E_k values. The codebooks are assumed to be complex Gaussian for all the users with $U_1 = U_2 = ... = U_M = CN(0, 1)$.

It is observed in Fig. 4.1 that using more phase values by increasing the number of digits provides performance improvements. For instance, using 4 phase values instead of 2 results in 0.5 bpcu increase for the number of base station antennas around 90-100. Also, increasing the number of antennas provides reduction in the MUI, and hence it increases the achievable rates.

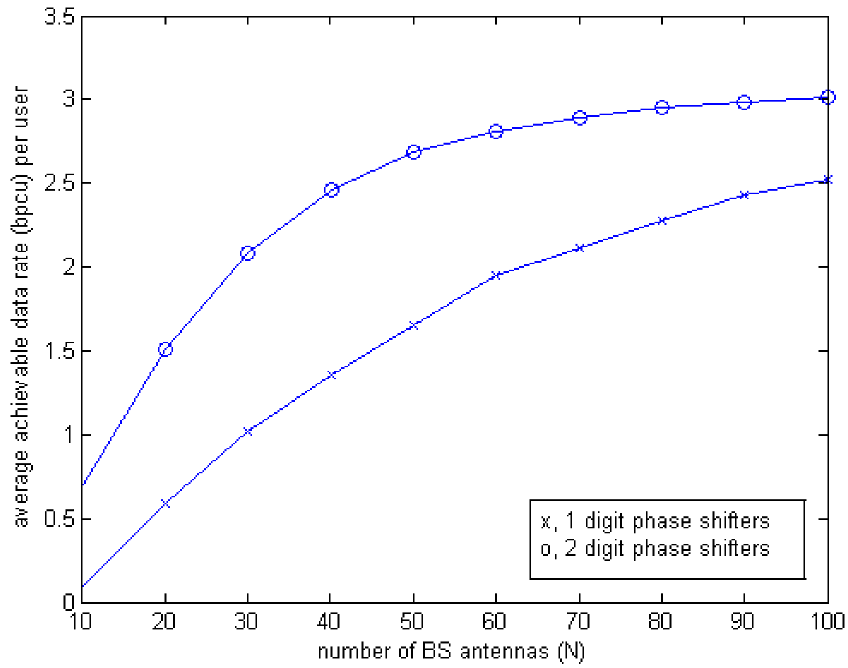

Figure 4.1: Average achievable data rate (in bpcu) versus the number of antennas for varying set of phase values over Rayleigh fading. $E_k = P_{BS} = 10$, $L = 2$, $M = 10$, $\sigma_w^2 = 1$.

We repeat the simulation in Fig. 4.1 with two digit PSs for different memory lengths including $L = 2$ and $L = 0$ (Greedy algorithm) in Fig. 4.2. We observe that employing the TB-CEP algorithm to determine transmission phases increases achievable rate by more than 0.2 bpcu per user (around 10% increase in achievable rates) for the number of BS antennas around 10 times the number of mobile terminals.

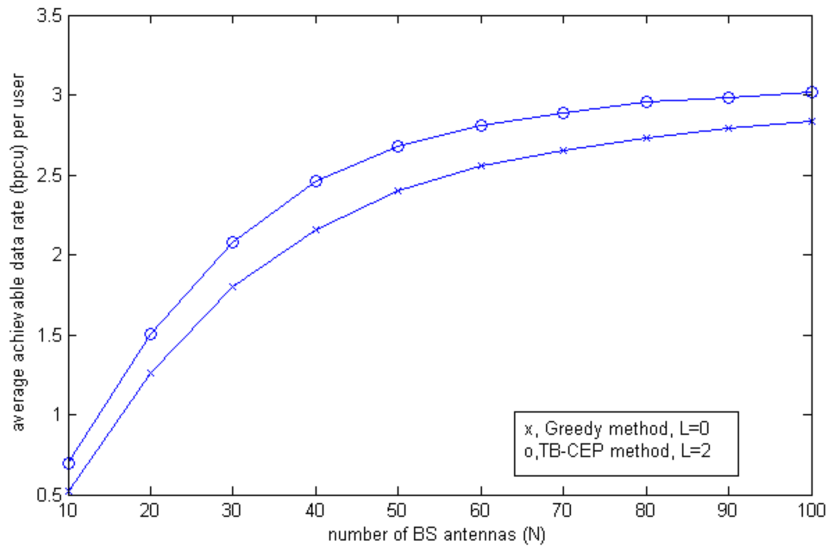

Figure 4.2: Average achievable data rate (in bpcu) versus the number of BS antennas over Rayleigh fading. $E_k = P_{BS} = 10$, $L = 2$, $M = 10$, $\sigma_w^2 = 1$

In [32], more extensive results including simulations of average per user achievable rates versus transmit power, number of trellis states, and errors in channel estimation and phase shifters can be found. It is observed that the performance of TB-CEP algorithm improves if the number of trellis states and the number of digits of PSs increase and is significantly affected by errors in channel estimation and non-idealities of phase shifters.

4.2 Discrete-Phase Multi Envelope Precoding for Massive MIMO Systems

Relaxing the CE constraint and allowing for multiple envelopes decreases the required BS power to provide a certain achievable data rate as it is shown in Chapter 3 for massive MIMO systems with continuous phase shifters. In this section, we adopt this multi-envelope precoding method for massive MIMO systems to the case of discrete phase shifters. We perform antenna grouping for splitting power before the phase angle determination stage as shown in Fig. 3.1 as solving both the phases and the envelopes together increases the complexity and then we determine the angles to be used for each antenna (as done in Chapter 3).

4.2.1 Antenna Grouping by Zero-Forcing

The vector of absolute values of the elements of the zero-forcing vector in (2.2), $\mathbf{v}_{abs} = [|v_{zf}^1|, |v_{zf}^2|, ..., |v_{zf}^N|]^T$ is used to group antennas as in the case of continuous phase shifters. The number of antenna groups depends on the number of PAs used at the BS and the number of antennas in each group is a design parameter which depends on the power ratios among the groups and the features of the PAs. The vector $\mathbf{p}_{zf}$ denotes the resulting power coefficient vector with $\mathbf{p}_{zf}^T\mathbf{p}_{zf} = N$ to satisfy the total transmit power constraint.

TB-CEP algorithm is a multi-stage method and the objective function in (4.4) has N real terms where the j^{th} term depends only on the first j variables. Therefore, we consider to reorder the antennas with the use of zero-forcing criterion before applying the TB-CEP algorithm in order to solve the transmit phase values. In this way, the signals of the antennas which need a higher envelope for transmission contributes on the minimization of more objective function variables as they are placed as the initial states.

Let $\hat{\mathbf{H}}$ be the reordered channel matrix where the first column is the channel realizations of the antenna which corresponds to the greatest absolute value at the zero-forcing vector $\mathbf{v}_{abs}$, and the N-th column consists of channel gains for the antenna corresponding to the least absolute value. Then, $\mathbf{p}_{zf}$ has the form of $[p_1...p_1, p_2...p_{a-1}, p_a...p_a]^T$ where a denotes for the number of PAs and $p_1 > p_2 > ... > p_a$, that is, we keep the power coefficient vector constant as we reorder $\mathbf{H}$.

4.2.2 Precoder Design

With the use of $\hat{\mathbf{H}}$ and $\mathbf{p}_{zf}$, the received signal for the k-th user is expressed as

$$y_k = \sqrt{\frac{P_{BS}}{N}} \hat{\mathbf{h}}_k \mathbf{\Lambda_{zf}} \mathbf{q} + w_k \tag{4.8}$$

where $\hat{\mathbf{h}}_k$ is the reordered channel vector to the k-th user, i.e., the k-th row of $\hat{\mathbf{H}}$ and $\mathbf{\Lambda}_{zf}$ is an $N \times N$ diagonal matrix with diagonal entries corresponding to elements of $\mathbf{p}_{zf}$. With the extraction of desired signal $\sqrt{E_k} u_k$ in (4.8), the received signal at the k-th user becomes

$$y_k = \sqrt{E_k} u_k + \left(\sqrt{\frac{P_{BS}}{N}} \hat{\mathbf{h}}_k \mathbf{\Lambda_{zf}} \mathbf{q} - \sqrt{E_k} u_k \right) + w_k. \tag{4.9}$$

This expression is very similar to the one in (4.2) except for the power coefficient vector. Then, the following nonlinear discrete optimization problem is formulated with the same strategy in Section 4.1.2 to minimize the sum of the MUI terms for all the users:

$$\begin{gathered} \mathbf{q} = \underset{\mathbf{q}}{\operatorname{argmin}} \sum_{j=1}^{N} Re \left(\sqrt{\frac{P_{BS}}{N}} \sum_{i=1}^{j-1} p_{zf}^j q_j^* \hat{\mathbf{G}}_{j,i} p_{zf}^i q_i - \mathbf{u}^H \mathbf{E} \hat{\mathbf{h}}_j p_{zf}^j q_j \right) \\ s.t.\ q_n \in Q_m, n = 1, 2, ..., N, \end{gathered} \tag{4.10}$$

where p_{zf}^j is the j-th term of power coefficient vector.

To solve for the nonlinear discrete optimization problem in (4.10) with a fast approach, Algorithm 5 can be used. However, the cumulative metric of the initial states and the branch metrics need to be calculated by using the reordered channel matrix and by taking the power coefficient vector into account. The cumulative metrics for all the initial states are calculated as follows

$$\sum_{j=1}^{L} Re\left(\sqrt{\frac{P_{BS}}{N}}\sum_{i=1}^{j-1} p_{zf}^{j} q_j^{*} \hat{\mathbf{G}}_{j,i} p_{zf}^{i} q_i - \mathbf{u}^H \mathbf{E} \hat{\mathbf{h}}_j p_{zf}^{j} q_j\right). \tag{4.11}$$

Calculation of the branch metric is performed by

$$Re\left(\sqrt{\frac{P_{BS}}{N}}\sum_{i=1}^{t+L-1} p_{zf}^{t+L} q_{t+L}^{*} \hat{\mathbf{G}}_{t+L,i} p_{zf}^{i} q_i - \mathbf{u}^H \mathbf{E} \hat{\mathbf{h}}_{t+L} p_{zf}^{t+L} q_{t+L}\right). \tag{4.12}$$

After the determination of the phase vector as summarized in Algorithm 5, the phase vector and the power coefficient vector are again reordered by the use of $\mathbf{v}_{abs}$ so that the phase and power coefficient values are picked for the actual antenna locations. Therefore, q_1 and p_{zf}^1 are used at the antenna corresponding to the greatest value in $\mathbf{v}_{abs}$, q_2 and p_{zf}^2 are used at the antenna with the second largest value in $\mathbf{v}_{abs}$, etc. Thus, the transmission phase vector, $\hat{\mathbf{q}}$ and the transmission power coefficient vector, $\hat{\mathbf{p}}_{zf}$ are determined. Through the use of this baseband (complex) signals, an achievable rate for the k-th user is calculated as follows [32]

$$R_k(\hat{\mathbf{q}}, \hat{\mathbf{p}}_{zf}) = log_2\left(\frac{E_k}{I_k(\hat{\mathbf{q}}, \hat{\mathbf{p}}_{zf}) + \sigma_w^2}\right). \tag{4.13}$$

Determination of the order of the antennas according to the zero-forcing algorithm and calculation of the phase angles to minimize the objective function is two serial stages. Ordering of antennas according to the zero-forcing vector includes calculating pseudo inverse of an $N \times M$ matrix which is of complexity $O(NM^2)$, and a matrix vector product which is of $O(NM)$ complexity. Calculating the transmission phases is similar to Algorithm 5, and has a complexity of $O(N^2Mm^{L+1})$ and reordering phase values and power coefficient has a complexity of $O(N)$. Therefore, the overall complexity of the multi-envelope precoding for massive MIMO systems with discrete phase shifters is around the same order as the TB-CEP algorithm.

4.2.3 Examples

In this section, we provide several numerical examples to compare the multi-envelope precoding method with the TB-CEP algorithm and CE precoding with continuous phase shifters.

We repeat the simulation in Fig. 4.1 and obtain achievable rate performance of the multi-envelope precoding algorithm with discrete phase shifters and TB-CEP algorithm versus the number of BS antennas for different number of supported phase values and different power coefficients in Fig. 4.3. As we have equal number of elements in each antenna group for multi-envelope precoding, power coefficients p_1 and p_2 satisfies $p_1 = \sqrt{2 - p_2^2}$ to keep the total transmit power the same.

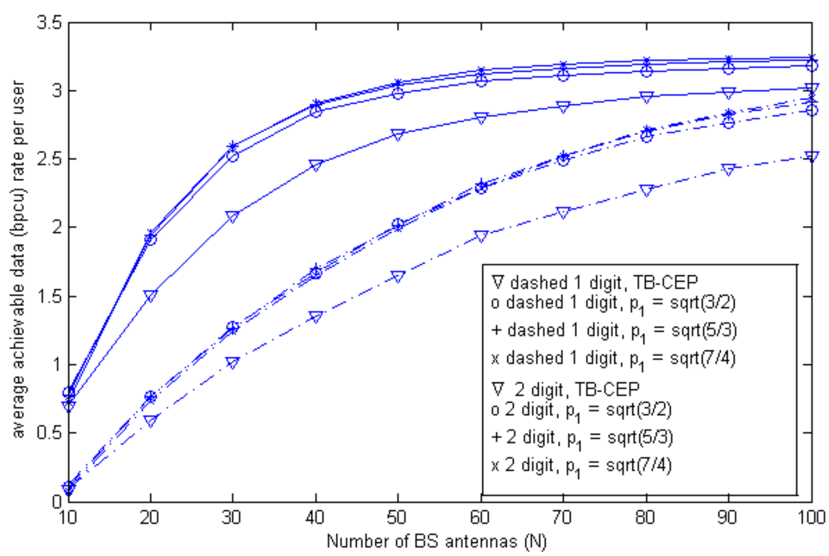

Figure 4.3: Average achievable data rate (in bpcu) versus the number of BS antennas over Rayleigh fading. $E_k = P_{BS} = 10,\ L = 2,\ M = 10,\ \sigma_w^2 = 1$

In Fig. 4.3, we observe that the newly proposed multi-envelope precoding technique outperforms the TB-CEP algorithm even when only 2 PAs are used. Its achievable rate performance is increased approximately 0.2 bpcu (around 10%) in the case of 2 digit PSs and 0.4 bpcu (around 20%) for 1 digit PSs for 70-100 base station antennas. Another way to see this improvement is that the performance of TB-CEP algorithm is achieved by using a smaller number of BS antennas with multi-envelope precoding. Furthermore, it does not seem to be necessary to optimize the power coefficients as the results with $p_1 = \sqrt{3/2}$, $p_1 = \sqrt{5/3}$ and $p_1 = \sqrt{7/4}$ are very similar.

We combine the simulation results in Fig. 4.3 and Fig. 2.3, and simulate a three-envelope precoding scheme with discrete phase shifters in Fig. 4.4. The power coefficient vector in the two-envelope case is selected as $\left[\sqrt{3/2}, ..., \sqrt{3/2}, \sqrt{1/2}, ..., \sqrt{1/2}\right]$, while the one in the three-envelope case is chosen as $\left[\sqrt{3/2}, ..., \sqrt{3/2}, 1, ..., 1, \sqrt{1/2}, ..., \sqrt{1/2}\right]$ where $\mathbf{p}_{zf}^T \mathbf{p}_{zf} = N$ is satisfied for both cases as antenna groups with equal number of elements are used.

We observe that increasing the number of antennas improves the achievable rate performance of all the algorithms. It is obvious through Fig. 4.4 that use of discrete phase shifters causes degradation in the performance compared to the case of continuous phase shifters as the number of phases is limited to a few values, however, it should be noted that working with discrete phase shifters is easier and robust for errors in the voltage control lines [36]. Furthermore, we observe that for the present setting the proposed multi-envelope precoding technique with discrete phase shifters is successful to close the gap between the TB-CEP algorithm and CE precoding with continuous phase shifters, that is, about half of the gap is removed with the use of only 2-3 PAs when 90-100 base station antennas utilized at the BS. We also note that, for this example, two-envelope precoding with continuous PSs does not provide such improvements in this case as the background noise is dominant as opposed to the remaining MUI energy and the user symbol energies are kept constant for all the

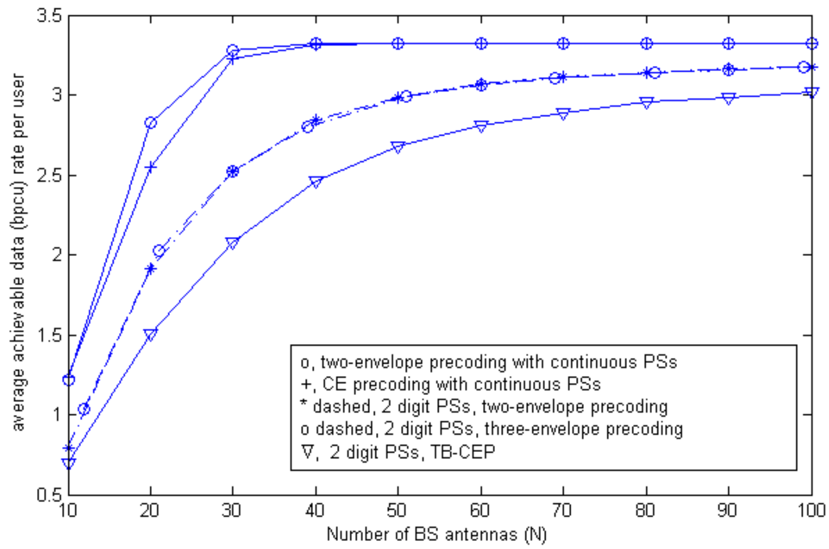

Figure 4.4: Average achievable data rate (bpcu) versus the number of antennas over Rayleigh fading. $E_k = P_{BS} = 10$, $L = 2$, $M = 10$, $\sigma_w^2 = 1$

algorithms. It is observed that beyond some point, with the use continuous phase shifters, system operates in the noise limited region, hence further increasing the number of antennas does not improve the achievable rate.

4.3 Chapter Summary

In this chapter, we have reviewed the use of discrete phase shifters for CE precoding in massive MIMO systems [32], and then we have applied the newly proposed multi-envelope precoding technique for this set-up. As in Chapter 3, we use the zero-forcing criterion in order to reorder the antennas before the (multi-stage) TB-CEP algorithm, and determine antennas requiring higher envelope levels. Through extensive simulations, we have shown that the use of 2-3 envelopes and antenna grouping with the zero-forcing algorithm provide significant benefits and partly recovers the gap between the performance of CE precoding with continuous phase shifters and that of TB-CEP algorithm for a noise limited scenario.

Chapter 5

Conclusions and Future Work

In this thesis, we have studied massive MIMO systems for wireless communications. Specifically, we have focused on reducing the hardware complexity of base stations in such systems, and to this end, we have proposed multi-envelope precoding techniques which utilize more than one (but only a few, e.g., 2-3) PAs. Our primary objective is to reduce the performance loss caused by CE precoding compared to the average only power constraint based precoding.

The proposed multi-envelope precoding technique with continuous phase shifters allows for the use of different envelopes for different groups of antennas. The solution of the zero forcing algorithm which utilizes both the channel state information and information symbols of all the mobile terminals is used to group the antennas with different signal envelope requirements. The number of the groups of antennas depends on the number of PAs used and groups of equal number of elements are generally considered, however, different designs are also possible. Through extensive simulations, it is demonstrated that the proposed multi-envelope precoding technique recovers some of the performance loss due to the CE precoding for both flat fading and frequency selective channels with the use of only a few, e.g., 2-3 PAs, hence it provides a more competitive spectral efficiency with respect to CE precoding. For example, for the case of 200 BS antennas serving 40 mobile users over flat fading channels, with the use of 2 PAs, the required power for an achievable rate of 2 (bpcu) decreases around 1 dB compared to CE precoding solutions.

The multi-envelope precoding technique is further extended to the case of discrete phase shifters and solutions based on trellis based constant envelope precoding of [32] are obtained. As done in the case of continuous phase shifters, the zero forcing algorithm is utilized to group the antennas requiring different envelope levels and to reorder the channel matrix before solving for the phase angles through the multi-stage TB-CEP algorithm. This is because, the j^{th} objective variable depends only on the first j variables thanks to the reformulation of the objective function developed for TB-CEP algorithm. This way, the antennas requiring higher envelopes participate in the solutions of more objective variables. The results show that the newly proposed multi-envelope precoding technique recovers some of the loss that is caused by the use of discrete phase shifters compared to CE precoding solutions utilizing continuous phase shifters. For instance, for the case of 90-100 antennas serving 10 mobile users over flat fading channels and $\frac{P_{BS}}{\sigma^2} = 10$, about half of the gap between achievable rates of CE precoding with continuous PSs and TB-CEP with 2 digit digital PSs is closed through the use of multi-envelope precoding with the same digital PSs and 2-3 PAs.

Massive MIMO is a recent topic of high interest with many subjects requiring further study. For instance, as an extension of the work in this thesis (and in the CE precoding literature), use of a smaller number of phase shifters can be considered to further decrease the hardware complexity of a BS. Also, noting that errors in phase shifters and channel estimation result in some loss in the performance of the algorithms, and currently these are not considered for the optimization of phase angles, another research direction for multi-envelope precoding is to take these into account to obtain more robust solutions. Furthermore, other techniques which do not use the transmitted data info that heavily can be explored for antenna grouping in order to decrease the number of switching operations between the PAs and for obtaining actual precoding solutions. The use of one bit ADCs can also be considered with CE precoding and multi-envelope precoding to further decrease the hardware costs of the base stations. Finally, we note that appropriate channel coding/modulation techniques with CE or multi-envelope precoding should be considered as future research.

Bibliography

[1] E. G. Larsson, O. Edfors, F. Tufvesson, and T. L. Marzetta, "Massive MIMO for next generation wireless systems," *IEEE Communications Magazine*, vol. 52, no. 2, pp. 186–195, Feb. 2014.

[2] T. L. Marzetta, "Noncooperative cellular wireless with unlimited numbers of base station antennas," *IEEE Transactions on Wireless Communications*, vol. 9, no. 11, pp. 3590–3600, Nov. 2010.

[3] W. Roh, J. Y. Seol, J. Park, B. Lee, J. Lee, Y. Kim, J. Cho, K. Cheun, and F. Aryanfar, "Millimeter-wave beamforming as an enabling technology for 5G cellular communications: theoretical feasibility and prototype results," *IEEE Communications Magazine*, vol. 52, no. 2, pp. 106–113, Feb. 2014.

[4] T. M. Duman and A. Ghrayeb, *Coding for MIMO Communication Systems*. West Sussex, UK: John Wiley & Sons, 2008.

[5] L. C. Godara, "Application of antenna arrays to mobile communications. II. beam-forming and direction-of-arrival considerations," *Proceedings of the IEEE*, vol. 85, no. 8, pp. 1195–1245, Aug. 1997.

[6] D. Tse and P. Viswanath, *Fundamentals of Wireless Communication*. London, UK: Cambridge University Press, 2005.

[7] M. Vu and A. Paulraj, "MIMO wireless linear precoding," *IEEE Signal Processing Magazine*, vol. 24, no. 5, pp. 86–105, Sep. 2007.

[8] G. Caire and S. Shamai, "On the achievable throughput of a multiantenna Gaussian broadcast channel," *IEEE Transactions on Information Theory*, vol. 49, no. 7, pp. 1691–1706, Jul. 2003.

[9] H. Weingarten, Y. Steinberg, and S. S. Shamai, "The capacity region of the Gaussian multiple-input multiple-output broadcast channel," *IEEE Transactions on Information Theory*, vol. 52, no. 9, pp. 3936–3964, Sep. 2006.

[10] E. Dahlman, S. Parkvall, J. Skold, and P. Beming, *3G Evolution, Second Edition: HSPA and LTE for Mobile Broadband*, 2nd ed. Massachusetts, USA: Academic Press, 2008.

[11] J. Berkmann, C. Carbonelli, F. Dietrich, C. Drewes, and W. Xu, "On 3G LTE terminal implementation - standard, algorithms, complexities and challenges," in *2008 International Wireless Communications and Mobile Computing Conference*, Crete Island, Greece, Aug. 2008, pp. 970–975.

[12] G. J. Foschini and M. J. Gans, "On limits of wireless communications in a fading environment when using multiple antennas," *Wireless personal communications*, vol. 6, no. 3, pp. 311–335, Mar. 1998.

[13] F. Rusek, D. Persson, B. K. Lau, E. G. Larsson, T. L. Marzetta, O. Edfors, and F. Tufvesson, "Scaling up MIMO: Opportunities and challenges with very large arrays," *IEEE Signal Processing Magazine*, vol. 30, no. 1, pp. 40–60, Jan. 2013.

[14] T. S. Rappaport, S. Sun, R. Mayzus, H. Zhao, Y. Azar, K. Wang, G. N. Wong, J. K. Schulz, M. Samimi, and F. Gutierrez, "Millimeter wave mobile communications for 5G cellular: It will work!" *IEEE Access*, vol. 1, pp. 335–349, May 2013.

[15] C. Shepard, H. Yu, N. Anand, E. Li, T. Marzetta, R. Yang, and L. Zhong, "Argos: Practical many-antenna base stations," in *Proceedings of the 18th Annual International Conference on Mobile Computing and Networking*, ser. Mobicom '12. New York, NY, USA: ACM, Aug. 2012, pp. 53–64.

[16] J. Vieira, S. Malkowsky, K. Nieman, Z. Miers, N. Kundargi, L. Liu, I. Wong, V. Öwall, O. Edfors, and F. Tufvesson, "A flexible 100-antenna testbed for massive MIMO," in *2014 IEEE Globecom Workshops*, Dec. 2014, pp. 287–293.

[17] L. Lu, G. Y. Li, A. L. Swindlehurst, A. Ashikhmin, and R. Zhang, "An overview of massive MIMO: Benefits and challenges," *IEEE Journal of Selected Topics in Signal Processing*, vol. 8, no. 5, pp. 742–758, Oct. 2014.

[18] F. Boccardi, R. W. Heath, A. Lozano, T. L. Marzetta, and P. Popovski, "Five disruptive technology directions for 5G," *IEEE Communications Magazine*, vol. 52, no. 2, pp. 74–80, Feb. 2014.

[19] H. Q. Ngo, E. G. Larsson, and T. L. Marzetta, "Energy and spectral efficiency of very large multiuser MIMO systems," *IEEE Transactions on Communications*, vol. 61, no. 4, pp. 1436–1449, Apr. 2013.

[20] J. Jose, A. Ashikhmin, T. L. Marzetta, and S. Vishwanath, "Pilot contamination and precoding in multi-cell TDD systems," *IEEE Transactions on Wireless Communications*, vol. 10, no. 8, pp. 2640–2651, Aug. 2011.

[21] F. Kaltenberger, H. Jiang, M. Guillaud, and R. Knopp, "Relative channel reciprocity calibration in MIMO/TDD systems," in *2010 Future Network Mobile Summit*, Florance, Italy, Jun. 2010, pp. 1–10.

[22] H. Zhang, S. Gao, D. Li, H. Chen, and L. Yang, "On superimposed pilot for channel estimation in multicell multiuser MIMO uplink: Large system analysis," *IEEE Transactions on Vehicular Technology*, vol. 65, no. 3, pp. 1492–1505, Mar. 2016.

[23] Y. Zhang, W. Feng, L. Dong, and N. Ge, "Pilot sequence design for multi-cell distributed MIMO systems with large-scale CSI," in *2015 IEEE International Conference on Communications (ICC)*, Londıon, UK, Jun. 2015, pp. 1739–1744.

[24] Z. Wang, C. Qian, L. Dai, J. Chen, C. Sun, and S. Chen, "Location-based channel estimation and pilot assignment for massive MIMO systems," in *2015 IEEE International Conference on Communication Workshop (ICCW)*, London, UK, Jun. 2015, pp. 1264–1268.

[25] C. K. Wen, Y. Wu, K. K. Wong, R. Schober, and P. Ting, "Performance limits of massive MIMO systems based on bayes-optimal inference," in *2015 IEEE International Conference on Communications (ICC)*, London, UK, Jun. 2015, pp. 1783–1788.

[26] S. L. H. Nguyen and A. Ghrayeb, "Compressive sensing-based channel estimation for massive multiuser MIMO systems," in *2013 IEEE Wireless Communications and Networking Conference (WCNC)*, Shanghai, China, Apr. 2013, pp. 2890–2895.

[27] R. R. Muller, L. Cottatellucci, and M. Vehkaperä, "Blind pilot decontamination," *IEEE Journal of Selected Topics in Signal Processing*, vol. 8, no. 5, pp. 773–786, Oct. 2014.

[28] H. Q. Ngo and E. G. Larsson, "EVD-based channel estimation in multicell multiuser MIMO systems with very large antenna arrays," in *2012 IEEE International Conference on Acoustics, Speech and Signal Processing (ICASSP)*, Kyoto, Japan, Mar. 2012, pp. 3249–3252.

[29] S. C. Cripps, *RF Power Amplifiers for Wireless Communications, Second Edition (Artech House Microwave Library (Hardcover))*. Norwood, MA, USA: Artech House, Inc., 2006.

[30] S. K. Mohammed and E. G. Larsson, “Per-antenna constant envelope precoding for large multi-user MIMO systems,” *IEEE Transactions on Communications*, vol. 61, no. 3, pp. 1059–1071, Mar. 2013.

[31] S. K. Mohammed and E. G. Larsson, “Constant-envelope multi-user precoding for frequency-selective massive MIMO systems,” *IEEE Wireless Communications Letters*, vol. 2, no. 5, pp. 547–550, Oct. 2013.

[32] M. Kazemi, H. Aghaeinia, and T. M. Duman, “Discrete-phase constant envelope precoding for massive MIMO systems,” *IEEE Transactions on Communications*, vol. 65, no. 5, pp. 2011–2021, May 2017.

[33] C. Risi, D. Persson, and E. G. Larsson, “Massive MIMO with 1-bit ADC,” *CoRR*, vol. abs/1404.7736, May 2014.

[34] H. Yin, Z. Wang, L. Ke, and J. Wang, “Monobit digital receivers: design, performance, and application to impulse radio,” *IEEE Transactions on Communications*, vol. 58, no. 6, pp. 1695–1704, Jun. 2010.

[35] N. Liang and W. Zhang, “Mixed-ADC massive MIMO,” *IEEE Journal on Selected Areas in Communications*, vol. 34, no. 4, pp. 983–997, Apr. 2016.

[36] “Microwave101 Phase Shifters,” https://www.microwaves101.com/encyclopedias/phase-shifters, accessed: 2017-06-03.

[37] T. Yoo and A. Goldsmith, “On the optimality of multiantenna broadcast scheduling using zero-forcing beamforming,” *IEEE Journal on Selected Areas in Communications*, vol. 24, no. 3, pp. 528–541, Mar. 2006.

[38] S. Vishwanath, N. Jindal, and A. Goldsmith, “Duality, achievable rates, and sum-rate capacity of gaussian MIMO broadcast channels,” *IEEE Transactions on Information Theory*, vol. 49, no. 10, pp. 2658–2668, Oct. 2003.